Earth Systems and Environment
https://doi.org/10.1007/s41748-025-00656-5

ORIGINAL ARTICLE

Explainable Machine Learning Insights into Wetland Dynamics and Carbon Storage in the Irtysh River Basin

Kaiyue Luo[1,2] · Alim Samat[1,3,6] · Tim Van de Voorde[4] · Weiguo Jiang[5] · Jilili Abuduwaili[1,3,6]

Received: 15 January 2025 / Revised: 25 April 2025 / Accepted: 5 May 2025

Abstract

Wetlands are vital for global carbon storage, yet face significant pressures. This study quantifies wetland landscape pattern changes and their impact on carbon storage in the transboundary Irtysh River Basin (IRB) from 2000 to 2020, identifies key landscape drivers, and projects future carbon storage under distinct scenarios for 2030. We utilized multi-temporal land cover data (GWL_FCS30), landscape metrics (Fragstats), the InVEST model for carbon storage estimation, interpretable machine learning (NGBoost coupled with SHAP analysis) to link landscape patterns to carbon dynamics, sensitivity analysis, and the PLUS model for scenario-based future projections (Natural Scenario - S1, Wetland Protection - S2, Wetland Degradation - S3). From 2000 to 2020, total wetland area increased by 10,417 km², primarily driven by marsh and swamp expansion, resulting in a net carbon storage increase from 2.827×10^8 tC to 2.885×10^8 tC (net gain: 5.8×10^6 tC). Sensitivity analysis revealed high responsiveness (Sensitivity Index = 10.812) of carbon storage to wetland area change. The NGBoost model accurately predicted carbon storage based on landscape metrics (MSE = 0.682, RMSE = 0.8259, MAE = 0.7811). SHAP analysis identified the aggregation index (AI), largest patch index (LPI), and number of patches (NP) as the most critical landscape predictors influencing carbon storage. Future projections for 2030 estimate total carbon storage at 3.229×10^8 tC under S1 (stabilization), increasing to 3.421×10^8 tC under S2 (protection), but declining sharply to 1.871×10^8 tC under S3 (degradation). Landscape structure, particularly aggregation and the extent of large patches, significantly influences wetland carbon storage in the IRB. Proactive wetland protection policies are crucial for enhancing and maintaining carbon sequestration capacity in this sensitive transboundary basin, contributing to regional climate change mitigation efforts.

✉ Alim Samat
alim_smt@ms.xjb.ac.cn

Kaiyue Luo
107552203698@stu.xju.edu.cn

Tim Van de Voorde
Tim.VandeVoorde@UGent.be

Weiguo Jiang
jiangweiguo@bnu.edu.cn

Jilili Abuduwaili
jilil@ms.xjb.ac.cn

1 State Key Laboratory of Ecological Safety and Sustainable Development in Arid Lands, Xinjiang Institute of Ecology and Geography, Chinese Academy of Sciences, Urumqi 830011, China

2 College of Geography and Remote Sensing Science, Xinjiang University, Urumqi 830017, China

3 China-Kazakhstan Joint Laboratory for Remote Sensing Technology and Application, Al- Farabi Kazakh National University, Almaty 050012, Kazakhstan

4 Department of Geography, Ghent University, Ghent 9000, Belgium

5 Beijing Key Laboratory for Remote Sensing of Environment and Digital Cities, Faculty of Geographical Science, Beijing Normal University, Beijing 100875, China

6 University of Chinese Academy of Sciences, Beijing 100049, China

Published online: 21 May 2025

Graphical abstract

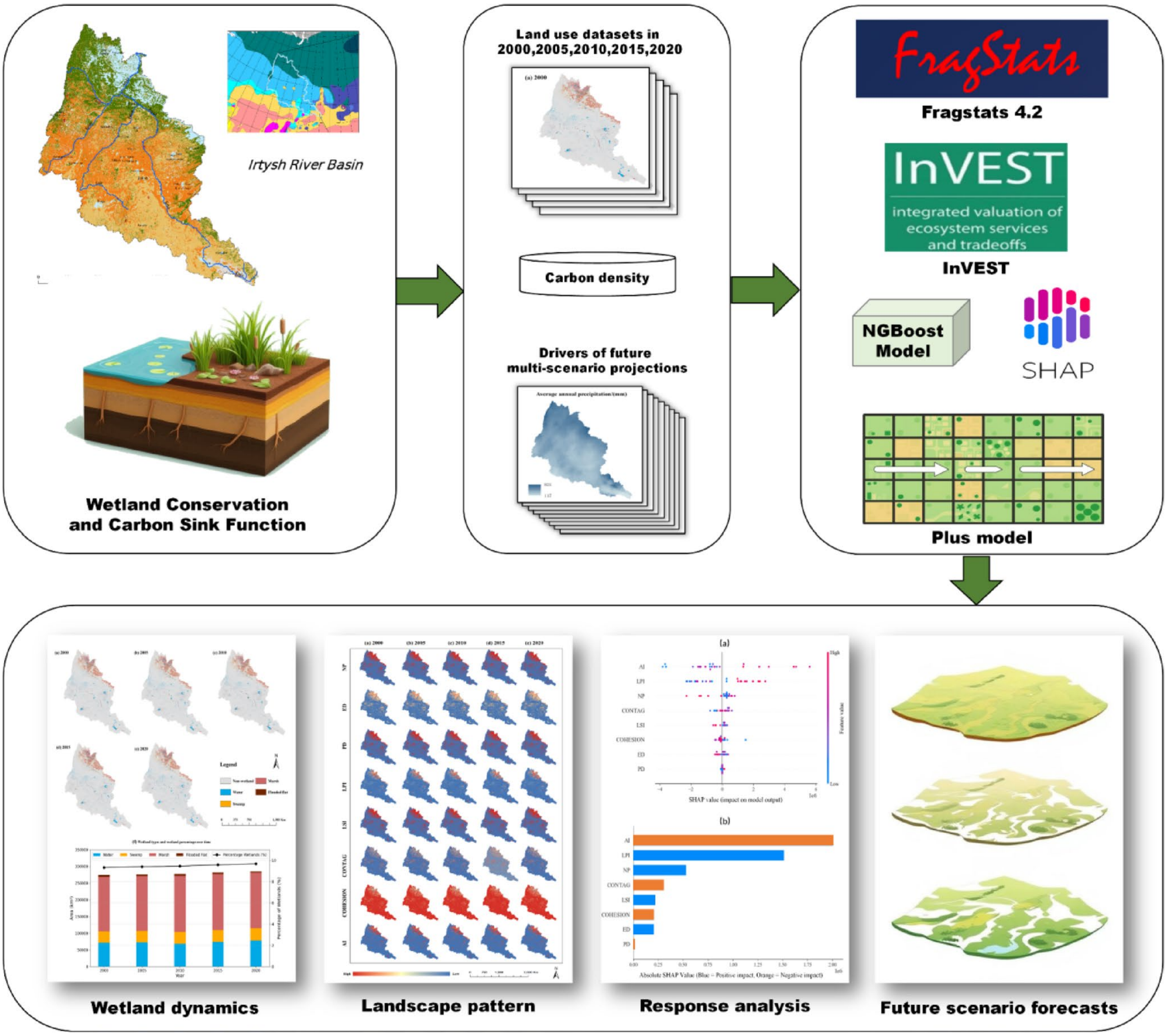

This graphical abstract summarizes a study on wetland dynamics and carbon storage in the Irtysh River Basin (IRB) from 2000 to 2020, with 2030 projections, focusing on wetland conservation and carbon sink roles. Using GWL_FCS30 land use data, Fragstats 4.2, InVEST, NGBoost with SHAP, and the PLUS model, the study analyzes landscape patterns, estimates carbon storage, identifies key drivers (e.g., aggregation index, largest patch index), and simulates future scenarios. Results show marsh and swamp expansion, increased fragmentation, and carbon storage rising to 2.885×10^8 tC by 2020. Projections for 2030 estimate 3.229×10^8 tC (Natural Scenario), 3.421×10^8 tC (Wetland Protection), and 1.871×10^8 tC (Wetland Degradation). This visual highlights the importance of wetland conservation for enhancing carbon sequestration and informs sustainable land-use strategies in transboundary basins

Keywords Wetland carbon storage · Landscape patterns · Irtysh river basin · InVEST model · Machine learning (SHAP) · Transboundary wetlands

1 Introduction

Wetlands are pivotal ecosystems that play multifaceted roles in global environmental processes, particularly in the carbon cycle. These ecosystems, characterized by water-saturated soils, support rich biodiversity and provide critical services such as water purification, flood control, and carbon sequestration (Davidson 2014). Globally, wetlands cover approximately 6-9% of the Earth's surface but store up to 35% of the global soil carbon, underscoring their role as significant natural carbon sinks (Gardner and Finlayson 2018). However, despite their ecological and climatic importance, wetlands are among the most threatened ecosystems. Climate change exacerbates sea level rise and alters precipitation patterns, leading to wetland degradation or loss. Human activities, such as agricultural expansion and urban development, further compound these threats, resulting in reduced biodiversity and impaired functionality (Zedler and Kercher 2005; Erwin 2009). Recent research has highlighted alarming rates of wetland loss in key regions around the world, with the impacts being particularly severe in regions experiencing rapid climatic shifts and anthropogenic pressures. For instance, in temperate and semi-arid regions, wetland degradation has been accelerated due to changes in precipitation patterns and increasing water demands for agriculture and urbanization (Fluet-Chouinard et al. 2023). Similarly, the widespread loss of wetlands in inland temperate zones has exacerbated the vulnerability of these ecosystems, with significant reductions in their capacity to store carbon and provide other ecosystem services (Murray 2023).

The Irtysh River Basin (IRB), spanning China, Kazakhstan, and Russia, represents a compelling and critical region where these wetland dynamics are particularly evident and understudied in the context of integrated landscape-carbon interactions. Located within the semi-arid temperate zone, the IRB functions as a vital hydrological and ecological system within a drought-vulnerable belt, making its wetland ecosystems highly susceptible yet globally relevant carbon stores. As part of an inland arid and semi-arid wetland system, these wetlands face intensifying pressures from both climatic variability (e.g., altered precipitation regimes) and pervasive human-induced land-use changes, rendering them especially sensitive to shifts in water availability and management practices (Huang et al. 2012; Wang et al. 2023a). The transboundary nature of the IRB significantly magnifies the complexity of environmental management, requiring coordinated international efforts for effective conservation (Woo et al. 2008; Sahana et al. 2024). Consequently, the basin's wetlands, which contribute substantially to both local livelihoods and global carbon storage, are subject to unique geopolitical and ecological challenges that complicate straightforward conservation solutions. The IRB's position in this drought-prone, fragile ecosystem zone, combined with its complex transnational governance structure, makes it an exemplary and urgent case for investigating how wetland landscape changes impact carbon sequestration capacity. Understanding these dynamics within the IRB is crucial not only for regional sustainability but also for informing broader climate regulation strategies and international policies aimed at mitigating climate change through nature-based solutions, highlighting the global significance of such regional deep-dives (Osland et al. 2017; Bellard et al. 2012).

In this context, the detailed study of landscape patterns becomes paramount for understanding carbon dynamics. Landscape patterns—the spatial arrangement and organization of various land uses and natural features—critically influence ecological processes, including nutrient cycling, biodiversity distribution, and particularly, carbon sequestration within wetland ecosystems (Du et al. 2025). Landscape ecology provides the essential theoretical framework for exploring how landscape structure affects ecosystem functions and services (Turner 1989). While various methods exist, the calculation of landscape metrics using tools like Fragstats offers a standardized and quantitative way to analyze landscape configuration (e.g., fragmentation, connectivity, shape complexity) and its potential impact on carbon sequestration processes (McGarigal et al. 2002). Although widely applied, quantifying these metrics is particularly crucial in heterogeneous and dynamic environments like the IRB, where changes in patch size, shape, and aggregation can significantly alter carbon fluxes (Hou et al. 2024b; Yuan et al. 2024). Wetland ecosystems, due to their saturated soils and diverse plant communities, are recognized as crucial carbon sinks, storing substantial amounts of carbon both in biomass and soils (Rogers et al. 2019). Traditional methods for estimating wetland carbon stocks rely on in situ observations, providing high-precision estimates of carbon stocks. However, these methods are costly in terms of financial, time, and human resources, and they are often limited to site-specific scales (Chmura et al. 2003). The rapid advancement of remote sensing (RS) technologies has provided a more efficient and accessible means for carbon stock estimation, allowing for large-scale and continuous monitoring. These developments have led to the emergence of model-based approaches for estimating carbon stocks, combining remotely sensed data with ecological models to improve the accuracy and scalability of carbon sequestration estimates. For example, Li et al. (2024) used a combination of RS data and process-based models to estimate carbon sequestration in coastal wetlands, highlighting the advantages of integrating multiple data sources for broader-scale carbon assessments (Wang et al. 2024).

In this study, the Integrated Valuation of Ecosystem Services and Tradeoffs (InVEST) model was employed to estimate carbon storage in the IRB. InVEST is widely recognized for its ability to integrate spatial, ecological, and economic data to simulate land-use dynamics and predict their impacts on ecosystem services, including carbon storage (Hamel et al. 2021). One of the primary advantages of InVEST over traditional methods is its ability to model ecosystem services under different land-use and climate scenarios, making it especially useful for future projections and scenario planning. Additionally, unlike earlier models that may rely solely on empirical data, InVEST incorporates a process-based approach that accounts for both biophysical factors and socio-economic influences, providing a more comprehensive analysis of carbon dynamics (Nelson et al. 2009). In contrast to CLUE-S or other static land-use models, which focus primarily on land-use allocation, InVEST allows for dynamic interactions between landscape patterns and ecosystem services. For example, He et al. (2016) used the InVEST model to evaluate the impact of urban expansion on regional carbon storage in China, demonstrating that the model could effectively integrate spatial, ecological, and economic data to simulate land-use dynamics and predict their impacts on carbon storage (He et al. 2016). In the context of the IRB, where wetlands are under intense pressure from human activities and climate variability, InVEST provides a valuable tool for assessing the impacts of wetland fragmentation on carbon storage. By modeling the carbon sequestration potential under current and projected future conditions, the model offers insights into how wetland restoration, conservation, or degradation can alter the carbon balance within the basin (Liu et al. 2018). These insights are essential for guiding land management practices and informing policy decisions, particularly in transnational basins like the IRB, where coordinated efforts are needed to mitigate the impacts of climate change on critical carbon sinks (Polasky et al. 2011).

Continuing from the introduction of landscape patterns and the InVEST model in assessing carbon storage changes, an exploration of the sensitivity of carbon storage to changes in wetland area is crucial. Sensitivity analysis is particularly pertinent as it highlights how small alterations in land use or ecological disturbances can disproportionately affect carbon sequestration capabilities. The sensitivity index (SI), which quantifies the response of carbon storage to a unit change in wetland area, can provide valuable insights into the resilience and vulnerability of these ecosystems to environmental changes. This kind of analysis is instrumental in forecasting the potential impacts of both natural disturbances and anthropogenic interventions, thereby enabling more strategic conservation planning (Zhang et al. 2023b).

Furthermore, to move beyond simple correlations and understand the complex, potentially non-linear relationships between landscape patterns and carbon storage, the application of advanced machine learning (ML) models combined with interpretability frameworks like SHapley Additive exPlanations (SHAP) offers significant advantages (Stupariu et al. 2022). While ML models such as XGBoost, LightGBM, CatBoost, and NGBoost are increasingly utilized in ecological studies for prediction (Chu et al. 2024; Zhou et al. 2024b), their strength lies in effectively processing complex, high-dimensional datasets to uncover intricate patterns often missed by traditional statistical methods. For instance, Zhou et al. (2024) effectively used an XGBoost-SHAP model to unravel non-linear impacts on ecosystem services (Zhou Hou et al. 2024a). Critically, for informing management, the integration of SHAP values provides a robust, theoretically grounded framework (game theory) for interpreting these "black box" models (Lai et al. 2023; Lundberg and Lee 2017). SHAP quantifies the contribution of each input feature (e.g., specific landscape metrics) to the model's prediction (e.g., carbon storage level) for each observation, offering instance-level and global explanations. This interpretability is crucial not only for enhancing model transparency and trust but, more importantly, for identifying the key landscape drivers influencing carbon storage dynamics specifically within the diverse wetland types and environmental gradients of the IRB. By pinpointing the most influential landscape features (e.g., patch aggregation vs. fragmentation), this approach can guide more targeted and effective management interventions for maximizing carbon sequestration (Stupariu et al. 2022).

In addition to modeling current wetland dynamics, the ability to project future land-use changes and their potential impacts on carbon storage is crucial for comprehensive ecosystem management. To this end, we employed the Patch-Generating Land Use Simulation (PLUS) model, a tool that integrates land expansion analysis strategy (LEAS) and cellular automata (CA). The PLUS model is designed to simulate and predict spatial and temporal changes in land use, which is particularly valuable in regions like the IRB, where wetlands face pressures from both climatic variability and anthropogenic activities. By incorporating various driving factors such as socio-economic development, environmental policies, and natural landscape features, the PLUS model enables more accurate forecasts of how land-use patterns may evolve under different scenarios (Guo et al. 2024). Several recent studies have demonstrated the utility of the PLUS model in forecasting future landscape dynamics. For example, Zhu et al. (2024) applied the PLUS model to assess the ecosystem service functions of wetlands in northeastern China, demonstrating the model's effectiveness in evaluating the impacts of land-use changes on wetland services, including carbon storage, soil retention, and habitat quality (Zhu et al. 2024). In our study, the PLUS model is applied to the IRB to simulate land-use changes under three future scenarios: Natural Scenario (S1), Wetland Protection Scenario (S2), and Wetland Degradation Scenario (S3). These scenarios allow for a detailed exploration of how different land-use strategies may affect wetland dynamics and, consequently, carbon storage potential in the basin (Wang et al. 2018).

This study, therefore, adopts an integrated approach, synergizing landscape pattern analysis, process-based carbon modeling, interpretable machine learning, and scenario simulation to provide a comprehensive assessment of how wetland landscape patterns influence carbon storage in the IRB. While each component method is established in its domain, combining the InVEST model for robust carbon storage estimation, advanced ML models with SHAP for uncovering and interpreting the key landscape drivers, and the PLUS model for simulating plausible future land-use trajectories under different policy assumptions, offers a more holistic and mechanistically informed perspective than typically achieved through siloed approaches. This integrated framework aims to provide actionable insights for navigating the complex trade-offs between development, conservation, and carbon sequestration in transboundary basins like the IRB, contributing to coordinated management strategies for climate change mitigation and adaptation (Fan et al. 2023; Chaplin-Kramer et al. 2024). Therefore, the main goal of this study is to provide a comprehensive assessment of wetland landscape dynamics and their impact on carbon storage within the complex transboundary IRB, leveraging an integrated modeling approach to bridge historical analysis with future projections. Specifically, this research aims to make the following key scientific contributions:

(1) Quantify and elucidate the spatiotemporal patterns of wetland landscape change and associated carbon storage variations in the IRB from 2000 to 2020, providing a crucial baseline understanding for this ecologically significant and sensitive region.

(2) Reveal the key landscape pattern drivers influencing wetland carbon storage dynamics by employing interpretable machine learning (NGBoost combined with SHAP), thus offering mechanistic insights beyond traditional correlative approaches into how landscape structure governs carbon sequestration in this semi-arid, transboundary context.

(3) Evaluate the potential future trajectories of wetland extent and carbon storage under distinct land-use policy scenarios (natural development, wetland protection, wetland degradation) using integrated scenario simulation (PLUS-InVEST), thereby generating policy-relevant, spatially explicit information to support sustainable wetland management and climate mitigation efforts in the IRB.

(4) Demonstrate the synergistic value of integrating remote sensing data, landscape ecological principles, process-based carbon modeling (InVEST), explainable AI (ML-SHAP), and land-use simulation (PLUS) for a holistic past-to-future assessment of ecosystem services in complex socio-ecological systems.

By achieving these goals, this study not only addresses critical knowledge gaps regarding wetland carbon dynamics in the IRB but also offers valuable insights and a methodological framework applicable to other transboundary basins and ecologically sensitive regions facing similar pressures from climate change and human activities. The findings underscore the vital role of targeted wetland conservation and management strategies in enhancing regional carbon sequestration potential and contributing to global climate change mitigation goals.

2 Materials and Methods

2.1 Study Area

The IRB is a significant hydrological corridor spanning China, Kazakhstan, and Russia (Fig. 1). Covering an area of 165×10^4 km², this extensive basin encompasses diverse ecosystems and climatic zones, ranging from the temperate semi-desert conditions in its upper reaches to the harsh continental climate in the middle and lower sections. The basin is characterized by considerable temperature fluctuations, particularly in the midstream and downstream areas (Huang et al. 2014). The IRB's ecological importance is reflected in its role as a habitat for a wide array of flora and fauna, many of which exhibit unique adaptations to the basin's varied environmental conditions (Li et al. 2024b). Geomorphologically, the basin presents distinct contrasts. The upper reaches of the IRB are dominated by the Altai Mountains, where permafrost and glacial systems play a crucial role in the hydrological cycle, generating runoff that sustains the midstream regions in Kazakhstan (Jiang et al. 2016). As the river descends into the lowland Siberian sedimentary basin, the landscape shifts markedly to flat, expansive terrains, underscoring the complex interrelationship between geological formations and hydrological processes (Radelyuk et al. 2022). The wetlands within the IRB are of particular ecological and climatological interest. These ecosystems serve as significant carbon sinks, contributing to the global carbon cycle by sequestering atmospheric carbon dioxide. Wetland carbon storage occurs primarily through biogeochemical processes that promote the accumulation of soil organic matter and biomass (Villa and Bernal 2018). However, these wetland ecosystems face increasing pressure from anthropogenic influences, including agricultural expansion,

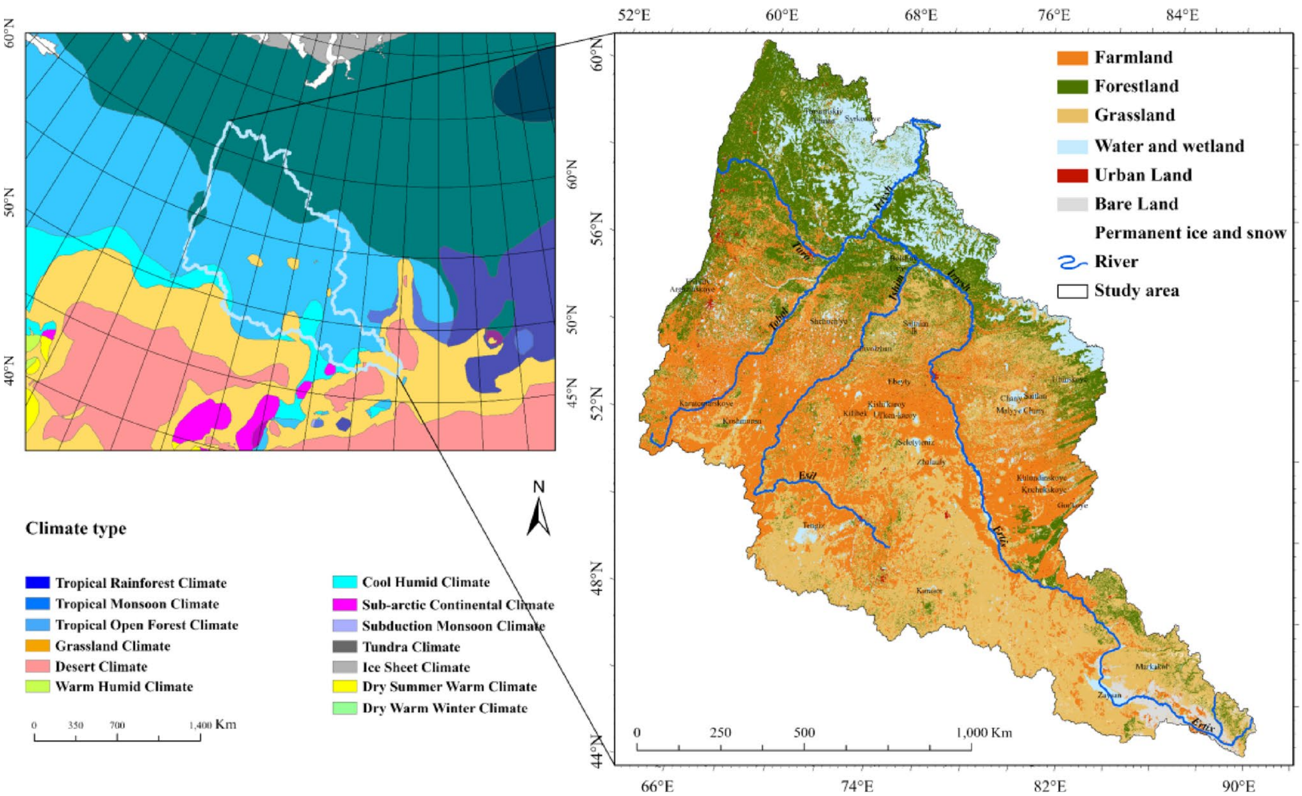

Fig. 1 Overview map of the study area: climate types for Coburn (left) and land use types for GLC_FCS30 in 2020 (right)

industrial development, and climate change-driven alterations in hydrological regimes and evapotranspiration (Luo et al. 2023).

2.2 Data Sources and Processing

This study analyzed the wetland dynamics of the IRB from 2000 to 2020 using the GWL_FCS30 dataset, which provides land use and land cover (LULC) data for five key time points: 2000, 2005, 2010, 2015, and 2020. With a spatial resolution of 30 m, the dataset incorporates a combination of Landsat optical data, Sentinel-1 Synthetic Aperture Radar (SAR) data, and ASTER Global Digital Elevation Model (GDEM) terrain data. This multi-source approach ensures comprehensive coverage of wetland features, with the dataset achieving an overall classification accuracy of 86% (Zhang et al. 2023a). In processing the dataset, we identified three main wetland types within the study area: swamp, marsh, and flooded flat. Swamps are characterized by the dominance of woody vegetation and are typically waterlogged for extended periods, making them significant carbon sinks due to the accumulation of organic matter in their saturated soils (de Araújo and Silveira 2024). Marshes, on the other hand, are herbaceous wetlands where standing or slow-moving water supports grasses and sedges, playing a crucial role in nutrient cycling and providing habitats for diverse species (Guthrie et al. 2022). Flooded flats, which are periodically inundated low-lying areas, contribute to flood control and groundwater recharge, reinforcing the ecological resilience of the basin (Meng et al. 2022). Additionally, we classified permanent water bodies, including rivers, lakes, and reservoirs, as part of the wetland system. Although these areas lack vegetation, their hydrological and ecological significance in maintaining the integrity of the wetland landscape justifies their inclusion as a distinct wetland category (Zhang et al. 2024).

The driving factors utilized for future multi-scenario projections of land use types include precipitation (PRE), temperature (TEM), digital elevation model (DEM), slope (SLO), aspect (ASP), NDVI, night-time light (NTL), population density (PD), and gross domestic product (GDP), as detailed in Table 1. Each dataset was carefully curated to capture key environmental, socioeconomic, and physical variables essential for the study. All data were resampled to a 1 km resolution with the Asia_North_Albers_Equal_Area_Conic projection.

2.3 Research Methods

Figure 2 presents the integrated methodological framework used to examine how wetland-landscape dynamics shape carbon storage in the IRB. The workflow advances through

Table 1 Introduction to driver factor raster data

Type	Driving factors	Description	Data sources
Land use	GWL_FCS30 dataset	At approximately 30 m spatial resolution, from 2000 to 2020	Zenodo (https://zenodo.org/records/6575731) (Zhang et al. 2023a)
Natural factors	PRE TEM	At approximately 4 km spatial resolution in 2020	TerraClimate (https://www.climatologylab.org/terraclimate.html) (Abatzoglou et al. 2018)
	DEM SLO ASP	Digital elevation model with 30 m spatial resolution Extracted from the DEM	Copernicus DEM (https://spacedata.copernicus.eu/collections/copernicus-digital-elevation-model)
	NDVI	At approximately 250 m spatial resolution in 2020	Terra MODIS NDVI (https://lpdaac.usgs.gov/products/mod13q1v061/)
Socio-economic factors	NTL	At approximately 500 m spatial resolution in 2020	Harvard Dataverse (https://doi.org/10.7910/DVN/YGIVCD) (Chen et al. 2020)
	PD	At approximately 100 m spatial resolution in 2020	WorldPop (https://www.worldpop.org/) (Sorichetta et al. 2015)
	GDP	Global 1 km × 1 km gridded revised real gross domestic product (million dollars) in 2019	Figshare (https://figshare.com/) (Chen et al. 2022a)

five stages. (1) Landscape pattern metrics were derived with Fragstats 4.2 from GWL_FCS30 wetland maps for each study year, quantitatively characterizing the spatial configuration of individual wetland classes. (2) Total wetland carbon stocks were estimated with the InVEST Carbon model by combining these maps with class-specific carbon-density values obtained from the literature. (3) A sensitivity analysis assessed how shifts in total wetland area between 2000 and 2020 influenced carbon storage. (4) To elucidate structure-function linkages, four ML algorithms—NGBoost, XGBoost, LightGBM and CatBoost—were trained with the landscape metrics as predictors and the InVEST-derived carbon stocks as the response. NGBoost outperformed the others and was interpreted with SHAP values to pinpoint the most influential landscape attributes. (5) Future change was explored with the PLUS model, which projected land use to 2030 under three scenarios: natural evolution (S1), wetland protection (S2) and wetland degradation (S3). The resulting maps fed back into InVEST to forecast scenario-specific carbon storage, thereby linking historical analysis to forward-looking assessments.

2.3.1 Landscape Pattern Index

To quantify the spatial structure of wetlands in the IRB and clarify its ecological significance for carbon storage, we derived a comprehensive set of landscape metrics with Fragstats 4.2. Guided by established links between landscape configuration and wetland carbon dynamics, we evaluated fragmentation and area using the number of patches (NP), patch density (PD), and the largest patch index (LPI), the latter indicating the dominance of the principal core wetland. Shape complexity was characterized by the landscape shape index (LSI) and edge density (ED), both sensitive to edge-driven processes that modulate carbon fluxes. Spatial aggregation and connectivity were captured through the contagion index (CONTAG), aggregation index (AI), and patch cohesion index (COHESION), where higher values generally reflect more continuous, less fragmented landscapes (Jia et al. 2019). All indices were computed at the landscape level for each GWL_FCS30-derived wetland map within the IRB boundary, yielding a temporally consistent record of wetland configuration. These metrics provide the quantitative basis for subsequent correlation analyses and machine-learning models that link landscape patterns to carbon-storage variability (Li et al. 2024a), detailed definitions and ecological interpretations are listed in Table 2.

2.3.2 Carbon Storage Assessment for Wetland Ecosystems

To reconstruct historical carbon stocks in IRB wetlands, we employed the Carbon Storage and Sequestration module of InVEST, which provides spatially explicit estimates at basin scale without the logistical burden of extensive field sampling. The workflow proceeded as follows. First, GWL_FCS30 LULC rasters for each study year were prepared as the primary spatial input. Second, we compiled a carbon-density table assigning literature-derived values (tC/ha) to four pools for each LULC type present in the IRB. While these uniform densities simplify modelling, they inevitably obscure local variability and thus constitute a recognized source of uncertainty.

The LULC raster and density table were then ingested by InVEST, which calculates cell-level carbon stock as:

$$C_{(i,j,M)} = A \times (D_a + D_b + D_c + D_d) \quad (1)$$

where A is the area of cell *(i, j)*. The model outputs a raster map of total carbon storage and a summary table for each year. Iterating this procedure across all time points yielded a consistent time series of carbon-storage maps for the IRB

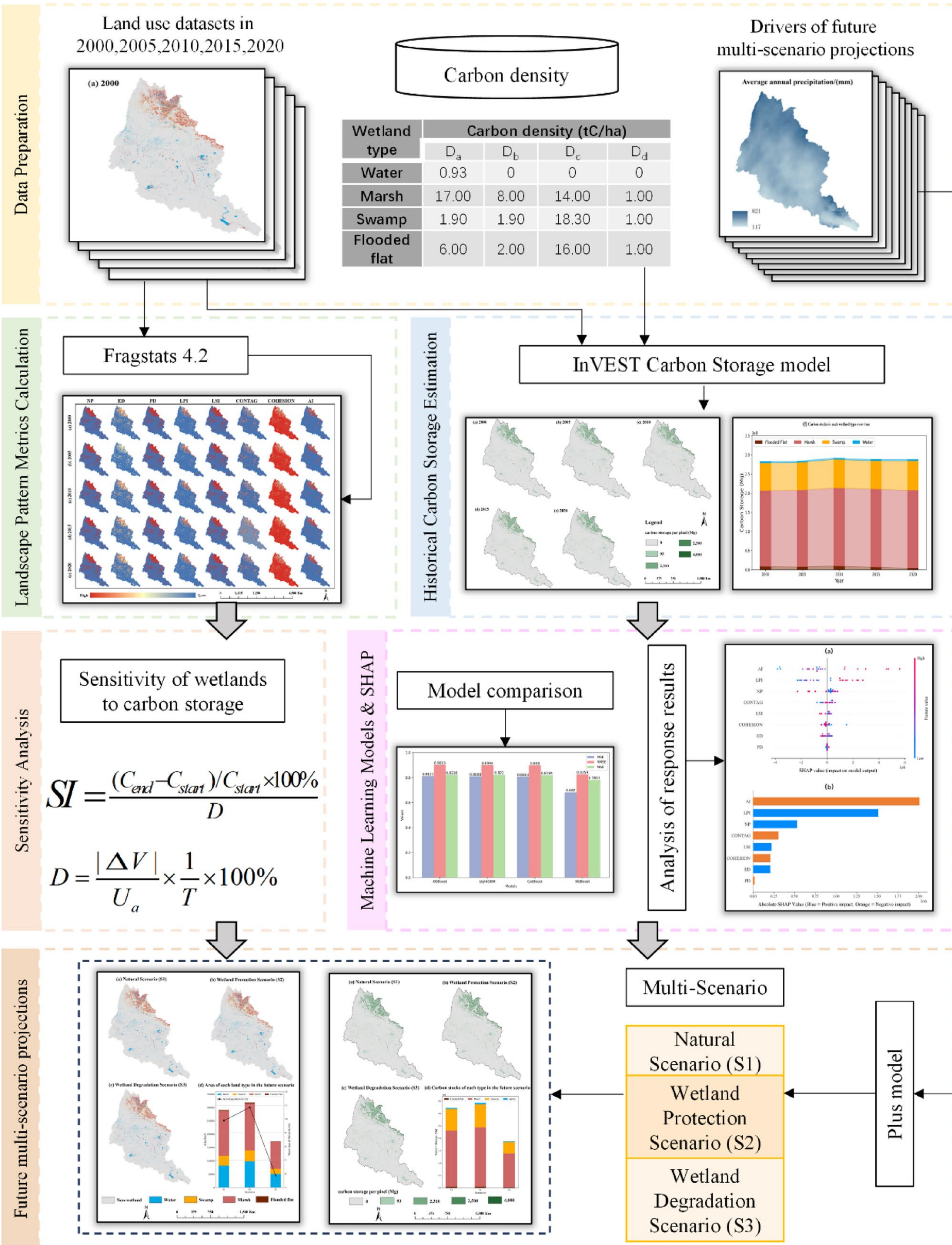

Fig. 2 Research framework

Table 2 Description and function of landscape metricss

Metrics	Abbreviation	Formula	Description
Number of Patches (Pcs)	NP	$\mathrm{NP} = \mathrm{N}$	The total number of patches in the landscape. N is the total number of patches in the landscape
Edge density ($\mathrm{m} \cdot \mathrm{ha}^{-1}$)	ED	$ED = \frac{\sum_{j=1}^{n} e^{ij}}{A}(10000)$	Total lengths of all edge segments involving the corresponding type divided by the total landscape area. e^{ij} is the length of j^{th} patch of type i;A represents landscape area
Patch density ($\mathrm{Pcs} \cdot \mathrm{ha}^{-1}$)	PD	$PD = \frac{N}{A}$	Number of patches of the corresponding type divided by total landscape area
Largest patch index (%)	LPI	$LPI = \frac{Max(a_i, ?a_n)}{A}(100)$	The percentage of the landscape composed of the largest patch. a_n is the number of patch of a landscape types
Landscape Shape Index	LSI	$LSI = \frac{0.25E}{\sqrt{A}}$	A measure of landscape shape complexity, comparing the total edge of the landscape to the minimum possible edge for the same area. E is the total length of the edges of the entire landscape
Contagion Index (%)	CONTAG	$CONTAG = [1 + \sum_{i=1}^{m} \sum_{j=1}^{n} \frac{P_{ij} \ln(P_{ij})}{2\ln(m)}](100)$	A measure of the degree of spatial aggregation of landscape patches of the same type. $i = 1, 2, \ldots, m$, is the type of landscape patches; $j = 1, 2, \ldots, n$, is the number of a certain patch landscape; P_{ij} is some types of patch number as a proportion of total patch
Patch Cohesion Index (%)	COHESION	$CONESION = [1 - \frac{\sum_{i=1}^{m} \sum_{j=1}^{n} P_{ij}}{\sum_{i=1}^{m} \sum_{j=1}^{n} P_{ij}\sqrt{a_{ij}}}][1 - \frac{1}{\sqrt{A}}]^{-1}(100)$	A measure of the degree to which patches of the same type are spatially cohesive, considering both their size and their perimeter
Aggregation Index (%)	AI	$AI = [\sum_{i=1}^{m} (\frac{g_{ii}}{\max g_{ii}})p_i](100)$	Measures the degree to which patches of the same type are spatially aggregated, considering their adjacency. g represents the number of pixels between different patches of the same patch type; p represents the proportion of landscape area occupied by each patch type

Table 3 Carbon-pool density

Wetland type	Carbon density (tC/ha)				References
	D_a	D_b	D_c	D_d	
Water	0.93	0	0	0	(Xiaomin et al. 2023)
Marsh	17.00	8.00	14.00	1.00	(Deng et al. 2022)
Swamp	1.90	1.90	18.30	1.00	(Zhang et al. 2023b)
Flooded flat	6.00	2.00	16.00	1.00	(Deng et al. 2022)

wetlands, forming the basis for subsequent trend analysis, sensitivity testing, and machine-learning modelling.

We need to input the carbon density parameters of different land use types into the InVEST model to estimate carbon storage, which includes the carbon densities of aboveground biomass (*Da*), belowground biomass (*Db*), soil organic matter (*Dc*), and dead organic matter (*Dd*) (Liu et al. 2019). The InVEST model methodology assumes a uniform carbon density for each land use category across the study area (Sharp et al. 2015). For this study, carbon density values for the four pools within each wetland type were derived from a synthesis of relevant previous research conducted in comparable environmental settings or geographical proximity, as detailed in Table 3. It is important to acknowledge that utilizing these literature-derived, constant values introduces inherent uncertainties into the carbon storage estimations. Real-world carbon densities can exhibit significant spatial heterogeneity within a large and diverse area like the IRB, influenced by local variations in factors such as soil properties, vegetation composition, hydrological regimes, and specific management practices. Therefore, while the model provides valuable insights into the overall magnitude, spatial distribution, and temporal trends of carbon storage, the absolute values should be interpreted with consideration of this limitation. Further localized field sampling and calibration would be necessary to refine the precision of these estimates.

To justify the selected literature values presented in Table 3, the characteristic ecological significance of each wetland type concerning carbon dynamics was considered. Swamps, typically dominated by woody vegetation and characterized by prolonged water saturation, generally foster conditions conducive to slow decomposition rates and significant accumulation of organic matter, particularly in soils, leading to relatively high carbon densities. Marshes, dominated by herbaceous plants, are often highly productive ecosystems contributing substantially to both aboveground and belowground biomass, as well as significant soil organic carbon pools. Flooded flats, being periodically inundated rather than permanently saturated, are expected to have lower organic matter accumulation and thus lower carbon densities compared to swamps and marshes, although still contributing to carbon storage. Permanent water bodies, lacking significant emergent vegetation and associated soil development, inherently possess the lowest carbon density among the studied wetland ecosystem components, primarily storing carbon within the water column or surface sediments. Therefore, the carbon density values compiled from previous studies (Table 3) reflect these expected relative differences based on the fundamental ecological characteristics and typical carbon cycling processes associated with each wetland type identified in the IRB.

2.3.3 Sensitivity Index Analysis Method

This study utilizes the SI to assess the impact of changes in wetland area on carbon storage (Zhang et al. 2023b). This index measures the response of carbon storage to a 1% change in wetland area (Peng et al. 2021; Qiu et al. 2021). A higher SI value indicates that carbon storage is more sensitive to changes in wetlands. When SI > 0, wetland changes have a positive impact on carbon storage; when SI < 0, the impact is negative. The expression is as follows:

$$SI = \frac{(C_{end} - C_{start})/C_{start} \times 100\%}{D} \tag{2}$$

$$D = \frac{|\Delta V|}{U_a} \times \frac{1}{T} \times 100\% \tag{3}$$

where *SI* is the Sensitivity Index, C_{start} and C_{end} represent the carbon storage at the beginning and end of the study period, respectively. D is the degree of wetland dynamics (%), ΔV representing the change in wetland type during the study period; U_a is the area of the wetland type at the beginning of the study; T is the duration of the study period.

2.3.4 Model Interpretation and Feature Importance Analysis

To delve deeper than simple correlations and understand the potentially complex, non-linear relationships driving carbon storage variations based on landscape structure within the IRB, we employed ML techniques followed by an interpretability analysis. The SHAP framework was used to clarify the decision-making processes of four advanced ML models: XGBoost, LightGBM, CatBoost, and NGBoost. SHAP, a game-theoretic method, assigns each feature an importance score that reflects its contribution to the model's output, providing an interpretable view of how landscape patterns influence carbon storage dynamics in wetlands (Lundberg and Lee 2017).

XGBoost is a distributed gradient boosting library optimized for efficiency, flexibility, and portability. It implements machine learning algorithms within a gradient boosting framework and offers parallel tree boosting, optimized for speed and performance (Chen and Guestrin, 2016). The objective function minimized by XGBoost is:

$$\mathcal{L}(\theta) = \sum_{i=1}^{n} \ell(y_i, \hat{y}_i) + \sum_{k=1}^{T} \Omega(f_k) \tag{4}$$

where $\ell(y_i, \hat{y}_i)$ represents the loss function (mean squared error), y_i is the observed target value, and $\hat{y}_i$ is the predicted value, T is the number of trees, and $\Omega(f_k)$ regularizes model complexity. In this study, the XGBoost model was configured with a learning rate of 0.02, 127 leaves per tree, a subsample rate of 0.7, and a column sampling rate of 0.6 to enhance model generalization.

LightGBM is a gradient boosting framework that employs tree-based learning algorithms, recognized for its efficiency in handling large datasets and its leaf-wise growth method, which helps prevent overfitting (Ke et al. 2017). The objective function is defined as:

$$F(x) = \sum_{i=1}^{n} \alpha_i f(x_i) \tag{5}$$

where *F(x)* is the model's output prediction, $f(x_i)$ is the weak learner for feature x_i, α_i represents the weight of the weak learner. For this study, LightGBM was configured with a learning rate of 0.02, 127 leaves per tree, feature fraction of 0.8, and bagging fraction of 0.9.

CatBoost is a gradient boosting library designed with a focus on handling categorical features. It combines decision trees and gradient boosting to create models that are resilient to overfitting and highly effective in processing categorical data(Prokhorenkova et al. 2018). The objective function is given by:

$$H(x) = \sum_{i=1}^{n} \alpha_i R_j(x_i) \tag{6}$$

where $H(x_i)$ represents the decision tree function of the input variables x_i, and $R_j(x_i)$ denotes the disjoint regions of the tree's leaves. In this study, CatBoost was set with a learning rate of 0.02 and a maximum tree depth of 6, with 1000 iterations.

NGBoost introduces a novel approach to gradient boosting by modeling the entire probability distribution of the output rather than predicting a single value. This probabilistic approach allows for a more detailed understanding and prediction of outcomes(Duan et al. 2020). NGBoost optimizes the following probabilistic objective function:

$$\mathcal{L}(P_\theta, y) = -\log P_\theta(y) \tag{7}$$

where $P_\theta(y)$ is the predicted probability distribution of the output y, and θ represents the parameters of the distribution. The NGBoost model was configured with 1000 estimators and a learning rate of 0.02, emphasizing its natural gradient approach to optimize probabilistic forecasts.

To evaluate the performance of these models, metrics such as Mean Absolute Error (MAE), Root Mean Squared Error (RMSE), and Mean Squared Error (MSE) were utilized. The model that demonstrated the highest performance, NGBoost, underwent feature importance analysis using SHAP. The SHAP value ϕ_i for feature i is calculated as follows:

$$\phi_i = \sum_{S \subseteq N \setminus \{i\}} \frac{|S|!(|N| - |S| - 1)!}{|N|!} [f(S \cup \{i\}) - f(S)] \tag{8}$$

where S is a subset of features, N is the set of all features, and $f(S)$ is the predicted outcome based on the subset S.

Additionally, the SHAP framework uses an additive feature attribution method to compute the SHAP value:

$$g(x') = \phi_0 + \sum_{i=1}^{M} \phi_i x'_i \tag{9}$$

Fig. 3 Driving factors

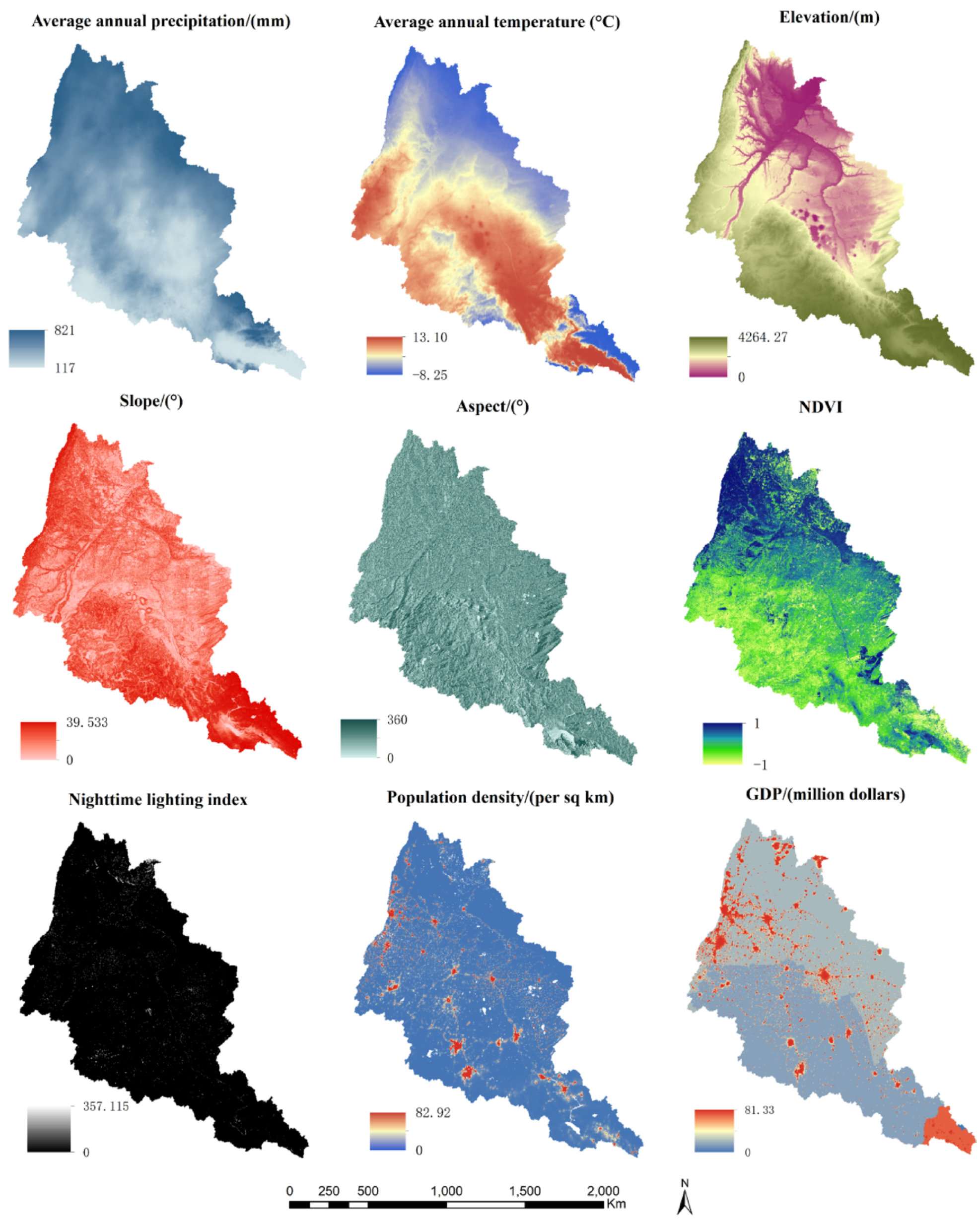

Table 4 Scenarios and principles for future land use change

Scenario	Land Use Change Principle
Natural Scenario (S1)	Natural land-use transitions driven by socioeconomic growth and climate (The binding effects of planning policies on land use change are not considered) (Nath et al. 2018)
Wetland Protection Scenario (S2)	Restriction of land conversion in wetlands with policy-driven restoration (Reduced transition probability of wetlands to non-wetlands by 50%. Increased probability of non-wetlands converting into wetlands by 20%. Water bodies remain stable or slightly increase) (Hou et al. 2024a)
Wetland Degradation Scenario (S3)	Intensified urban and agricultural development leading to wetland loss (Increased transition probability of wetlands to non-wetlands by 50%. Reduced probability of non-wetlands converting into wetlands by 20%. Water bodies remain stable or slightly reduce) (Qiu et al. 2022)

Table 5 Transfer matrix

	S1					S2					S3				
	A	B	C	D	E	A	B	C	D	E	A	B	C	D	E
A	1	1	1	1	1	1	1	1	1	0	1	0	0	0	1
B	1	1	1	1	1	1	1	1	1	0	0	1	0	0	1
C	1	1	1	1	1	1	1	1	1	0	0	0	1	0	1
D	1	1	1	1	1	1	1	1	1	0	0	0	0	1	1
E	1	1	1	1	1	1	1	1	1	1	0	0	0	0	1

A. Water Bodies, B. Swamps, C. Marshes, D. Flooded Flats, E. Non-wetlands. 0 means conversion to another land type is prohibited, and 1 means conversion to another land type is allowed.

where $g(x')$ is the interpretation model, ϕ_0 is the base value representing the average prediction, ϕ_i is the contribution of the i-th feature, $\mathbf{x}'_i$ indicates whether feature i is included or excluded, and M is the total number of features.

2.3.5 PLUS Model

To anticipate wetland trajectories and their carbon implications in the IRB to 2030, we applied the PLUS model, which couples the land-expansion analysis strategy (LEAS) with a cellular automaton using random patch seeding (CARS) (Liang et al. 2018). Historical LULC rasters for 2015 and 2020, derived from the GWL_FCS30 product, served both for calibration and as the simulation baseline. Nine biophysical and socio-economic drivers (Table 1; Fig. 3).

The LEAS module identifies land use expansion by extracting spatial patterns of site-level transitions over time and quantifying their probability using the Random Forest Classifier (RFC) algorithm (Li et al. 2012). This algorithm processes different driving factors independently for each land use type to determine its probability of expansion, providing insights into the relative importance of each factor in land transformation (Maxwell et al. 2019). The CARS module, on the other hand, incorporates both top-down (land demand) and bottom-up (land competition) mechanisms to simulate the patch evolution of land use across different scenarios (Xu et al. 2019a). This module employs a threshold-decreasing mechanism based on a Monte Carlo simulation to account for local neighborhood effects in land competition (Wu 1998).

Factors affecting future urban development and land-use change are multifaceted, and it is therefore important to take full account of various environmental factors when modeling and forecasting land-use change (Chen et al. 2022b). The following three scenarios were set up to explore future land use trends in a rational manner:

(1) Natural Scenario (S1): assumes no significant policy intervention, allowing natural dynamics and anthropogenic influences to shape land use.

(2) Wetland Protection Scenario (S2): prioritizes the protection and restoration of wetlands, enforcing stricter conservation policies to reduce land conversion in critical areas (Van Asselen and Verburg 2013).

(3) Wetland Degradation Scenario (S3): represents increased pressure on wetlands due to urban expansion, agricultural intensification, and reduced conservation efforts (Verburg et al. 2004).

The principles guiding land use change under these scenarios are outlined in Table 4, which shows the assumptions and key drivers for each scenario.

For each scenario, land use transfer matrices were developed to quantify the likelihood of transitions between different land use categories. These transfer matrices (Table 5) reflect the probability of conversion from one land type to another under each scenario, highlighting the potential risks or benefits to wetland areas (Li et al. 2020).

Domain weights indicate the expansion capacity of different land use types, and the amount of change in the area

Table 6 Neighborhood weight of each variety according to ΔTA

Variety	Non-wetlands	Water Bodies	Swamps	Marshes	Flooded Flats
ΔTA	− 3877	6073	363	− 540	− 2019
weight	0.01	1.00	0.43	0.34	0.19

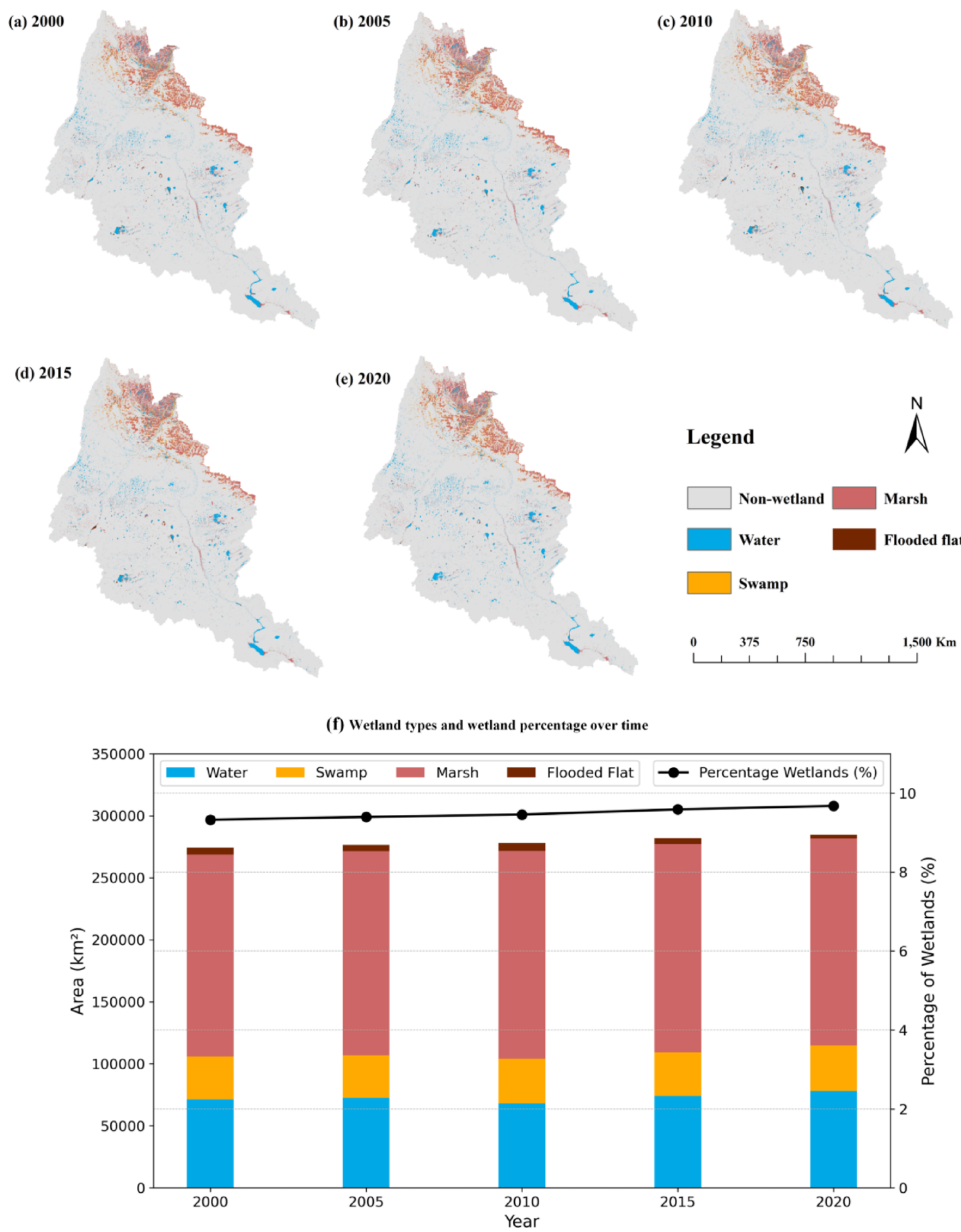

Fig. 4 Spatiotemporal dynamics of wetland distribution (**a**-**e**); Wetland area statistics by type(f)

Table 7 Wetland area statistics

Year	Wetland area by type(km²)					Total wetland area(km²)	Percentage of wetlands(%)
	Non-wetland	Water	Swamp	Marsh	Flooded flat		
2000	2665882.25	71215.72	34475.64	162938.06	5710.19	274339.61	9.33
2005	2663857.62	72388.92	34567.40	164513.48	4894.64	276364.44	9.40
2010	2662098.23	68049.01	36120.32	167479.75	6475.06	278124.15	9.46
2015	2658266.85	74128.77	35071.76	168244.78	4509.93	281955.25	9.59
2020	2655465.06	77970.62	36942.16	166799.89	3043.88	284756.56	9.68

(TA) of each land use type in the same time scale is more reflective of its expansion capacity, and in this study, we use the dimensionless value of ΔTA from 2015 to 2020 to determine the domain weights (Table 6), which are calculated by the following formula:

$$w_i = \frac{\Delta TA_i - \Delta TA_{\min}}{\Delta TA_{\max} - \Delta TA_{\min}} \tag{10}$$

where ΔTA_i is the change in area of expansion for each class; ΔTAm_{in} is the minimum value of change in area of expansion for each class; and ΔTA_{max} is the maximum value of change in area of expansion for each class.

3 Results

3.1 Changes in Landscape Patterns

From 2000 to 2020, the wetland area in the IRB increased from 274,339.61 km² (9.33% of the total land area) to 284,756.56 km² (9.68%), a net gain of 10,416.95 km² (Fig. 4; Table 7). This expansion, primarily driven by increases in swamps (+2,466.52 km²) and water bodies (+6,754.90 km²), reflects successful conservation efforts, hydrological recovery, or land-use shifts favoring wetland restoration. However, the modest decline in flooded flats (-2,666.31 km²) suggests localized pressures, possibly from agricultural intensification or altered flood regimes. This heterogeneous wetland dynamics sets the stage for understanding carbon storage changes, as wetland types like swamps and marshes are critical carbon sinks due to their high organic matter accumulation (Bridgham et al. 2006).

The breakdown of wetland types shows varied changes across the different categories (Table 7). Water bodies

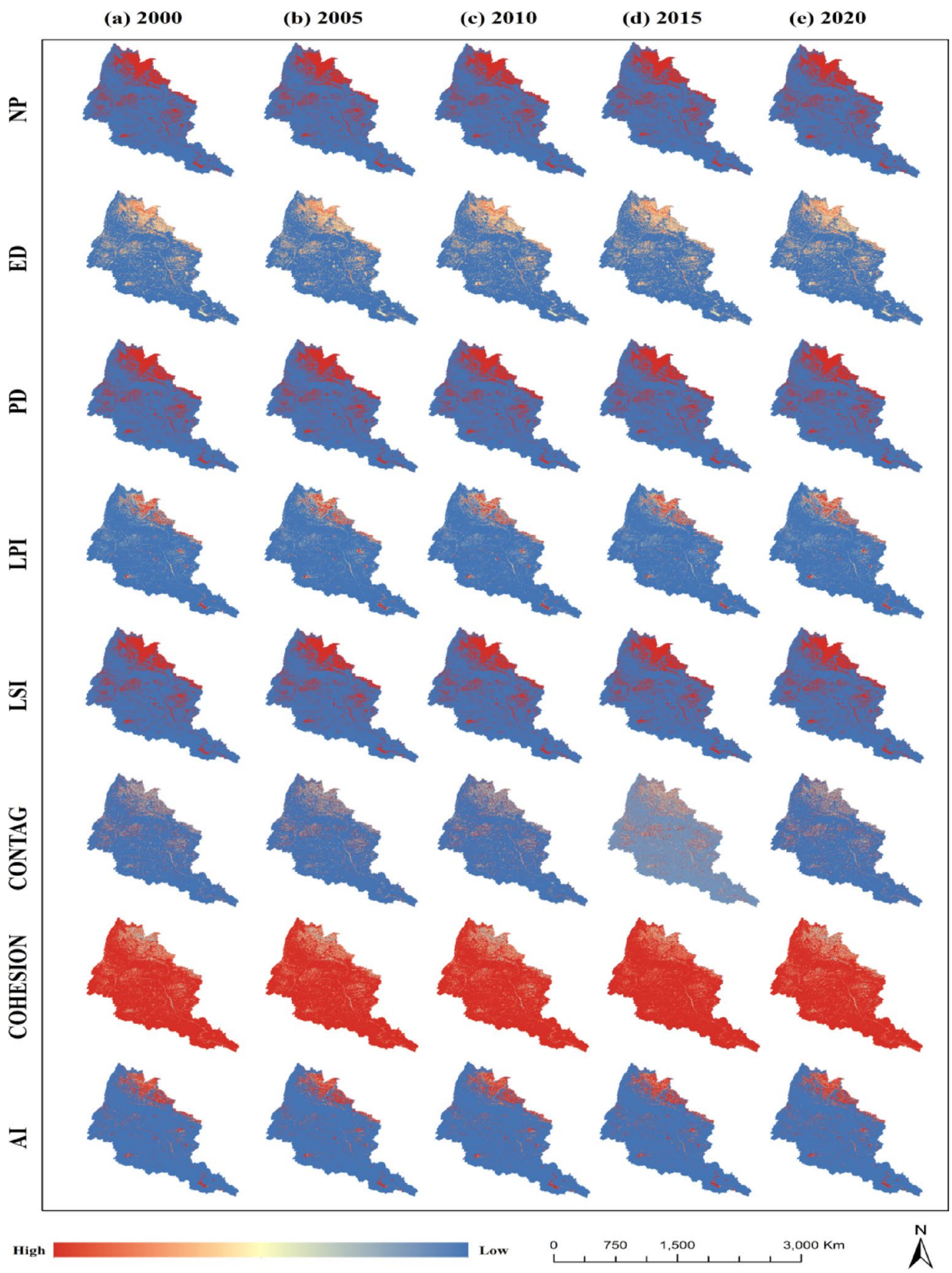

Fig. 5 Wetland landscape patterns

Table 8 Landscape pattern indexes

Year	NP	ED	PD	LPI	LSI	CONTAG	COHESION	AI
2000	15,744	0.4285	0.0033	0.7184	132.8145	61.9399	99.8940	65.6419
2005	15,753	0.4319	0.0033	0.7250	133.3540	61.8926	99.8942	65.6424
2010	15,912	0.4334	0.0033	0.7597	133.6374	61.8692	99.8948	65.6750
2015	16,567	0.4446	0.0035	0.8001	136.0410	64.5903	99.9063	65.3289
2020	16,800	0.4441	0.0035	0.7933	135.0433	61.7163	99.8923	65.7339

expanded from 71,215.72 km² in 2000 to 77,970.62 km² in 2020. Swamps also increased in area, growing from 34,475.64 km² to 36,942.16 km² over the same period. Marshs saw a modest increase, from 162,938.06 km² in 2000 to 166,799.89 km² by 2020. However, flooded flats experienced a notable decrease, shrinking from 5,710.19 km² in 2000 to 3,043.88 km² in 2020, indicating possible shifts in hydrological dynamics or floodplain management.

To further examine the spatial variability of landscape pattern indices, a sliding window method with a window size of 2000 was employed (Fig. 5). This method enables the visualization of landscape patterns across the study area. By applying this approach, localized trends and variations in landscape metrics are captured, offering a more detailed insight into the spatial structure and heterogeneity within the landscape. The 2000-unit window size ensures that the analysis remains sensitive to small-scale variations while still being relevant at the broader landscape scale.

Landscape pattern indices (Table 8) reveal significant structural changes in IRB wetlands from 2000 to 2020, with implications for ecosystem functionality. The NP rose from 15,744 to 16,800, and ED increased from 0.4285 to 0.4441 m/ha, indicating progressive fragmentation. This trend, likely driven by land-use pressures or hydrological variability, may reduce wetland connectivity, potentially impairing carbon sequestration efficiency (Nahlik and Fennessy 2016). Conversely, the LPI increased slightly from 0.7184 to 0.7933%, suggesting that dominant wetland patches remain intact, which is critical for maintaining carbon storage capacity. The AI also showed a marginal increase (65.6419–65.7339%), implying stable spatial cohesion despite fragmentation. These patterns directly inform subsequent carbon storage assessments, as larger, more aggregated patches typically enhance carbon sequestration by reducing edge-related carbon losses (Fickas et al. 2016). The PD remained relatively stable throughout the study period. While this reflects some constancy in the distribution of wetland patches per unit area, the rise in NP and ED suggests that these wetlands are becoming more fragmented, with new edges forming, possibly driven by shifts in hydrology or human activities (Fluet-Chouinard et al. 2023). The LPI showed a peak in 2015 at 0.8001% before declining slightly to 0.7933% in 2020, indicating that during this period, the most dominant wetland patch became larger and more prominent. This was accompanied by an increase in the LSI, which peaked in 2015, suggesting more complex and irregular wetland patch shapes during this time. The CONTAG initially rose from 61.9399% in 2000 to 64.5903% in 2015, implying greater aggregation or clustering of wetland areas. However, the subsequent decline to 61.7163% in 2020 indicates a return towards greater fragmentation, possibly driven by external pressures reducing the connectivity of wetland patches. COHESION remained remarkably high and stable across the entire period, consistently around 99.89%, reflecting that, despite fragmentation, the overall connectivity of the wetland landscape remains largely intact. This suggests that the wetlands, while becoming more fragmented in terms of patch structure, still maintain their ecological integrity and are not entirely isolated from one another. Lastly, the AI also exhibited stability, fluctuating around 65.6%. This consistency implies that, despite fluctuations in individual patch metrics, the degree of aggregation within wetland types has not experienced major changes over time.

3.2 Carbon Storage Changes

The analysis of carbon storage in the IRB wetlands over the period from 2000 to 2020 shows variations across different wetland types, including water bodies, swamps, marshes, and flooded flats (Fig. 6). The data presented in Table 9 highlights the changes in carbon storage in these wetland ecosystems.

From 2000 to 2020, carbon storage in the wetlands of the IRB exhibited noticeable fluctuations across different wetland types. The total carbon storage increased from 2.827×10^8 tC in 2000 to 2.885×10^8 tC in 2020, reflecting an overall growth of approximately 5.8×10^6 tC over the two-decade period. This increase in carbon storage is closely tied to both the expansion of wetland areas and the differing carbon densities of the various wetland types, as captured by the InVEST model.

The wetland types contributing most to this increase are marshes and swamps. Marshes, which consistently accounted for the largest portion of the wetland area, were the dominant contributors due to their relatively high carbon density—particularly in aboveground biomass (17.00 tC/ha) and soil organic matter (14.00 tC/ha). Despite only

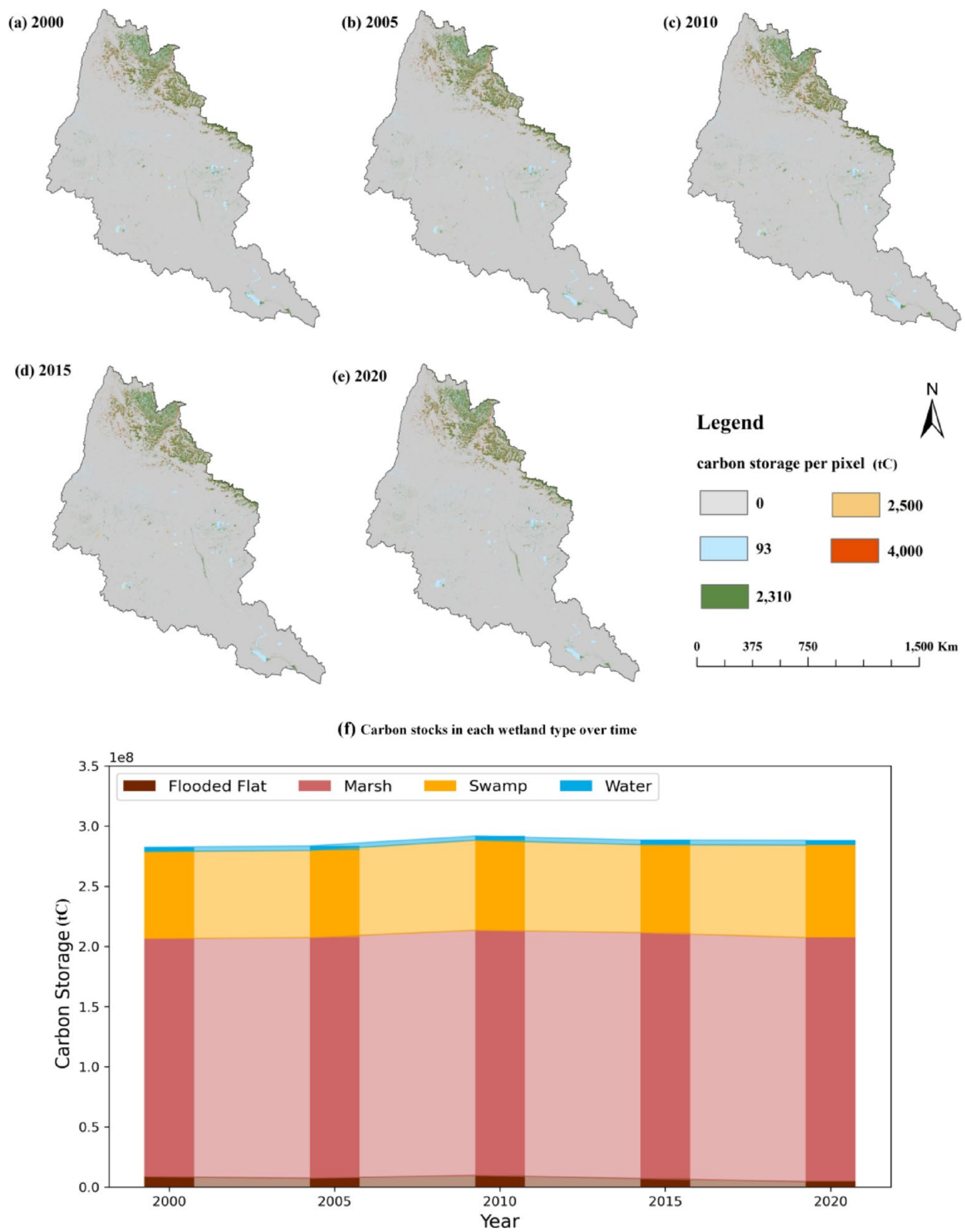

Fig. 6 Spatial and temporal dynamics of wetland carbon stock distribution (**a-e**); Wetland carbon stock statistics (f)

Table 9 Carbon storage (tC) by wetland type from 2000 to 2020

Year	Water	Swamp	Marsh	Flooded flat	Total
2000	3,819,882	72,284,000	197,849,190	8,717,500	282,670,572
2005	3,887,493	72,296,000	200,015,970	7,507,500	283,706,963
2010	3,654,249	74,688,000	203,790,510	9,837,500	291,970,259
2015	3,985,701	73,052,000	204,395,730	7,197,500	288,630,931
2020	4,209,831	76,780,000	202,787,970	4,695,000	288,472,801

moderate expansion in area, the large carbon pool associated with marshlands has had a substantial impact on total carbon sequestration. Swamps, though covering a smaller area than marshes, played an outsized role in carbon storage due to their high soil organic carbon density (18.30 tC/ha). Over the two decades, swamps saw a gradual increase in area, contributing significantly to the overall rise in carbon stocks. The elevated carbon density of swamps, particularly in soil organic matter, made them key to the basin's enhanced carbon sequestration, despite their relatively smaller coverage. Water bodies, though characterized by low carbon density (0.93 tC/ha), also contributed to the increase in carbon storage due to their expansion in area. However, their impact on overall carbon stocks was limited by their lack of substantial belowground, soil, or dead organic carbon pools. In contrast, flooded flats experienced a marked decline in area, shrinking from 5.71×10^3 km² in 2000 to 3.04×10^3 km² in 2020. This contraction, coupled with their relatively high soil organic matter density (16.00 tC/ha), resulted in a reduction of their contribution to total carbon storage. The loss of flooded flats may reflect changes in hydrological conditions or land use practices, which likely hindered their ability to maintain previous levels of carbon sequestration.

The overall increase in carbon stocks can therefore be attributed to the expansion of swamps and marshes, both of which possess significant carbon storage capacity in their biomass and soils. The InVEST model highlights that the high carbon density of these wetland types, particularly in soil organic matter, was a major factor driving the increase in carbon sequestration during this period. Maintaining and expanding these key wetland types, especially marshes and swamps, is critical to further enhancing the carbon storage capacity of the IRB.

3.3 Sensitivity of Wetlands To Carbon Storage Changes

To assess the sensitivity of carbon storage to wetland area changes in the IRB, we calculated the SI over the period from 2000 to 2020, yielding a value of 10.812. This high SI indicates that a 1% change in wetland area results in a disproportionately large change in carbon storage, highlighting the exceptional responsiveness of IRB wetlands to variations in their extent. For example, the observed 3.79% increase in wetland area (from 274,339.61 km² to 284,756.56 km²) corresponds to a 2.05% rise in carbon storage (from 2.827×10^8 tC to 2.885×10^8 tC), aligning with the SI's prediction of amplified carbon responses. This sensitivity is driven by the high carbon sequestration capacity of marshes and swamps, which dominate the IRB's wetland landscape and store significant organic carbon in their soils and biomass (Deng et al. 2022). The positive SI underscores the potential of wetland restoration to enhance carbon sequestration, as larger wetland areas, particularly those with high LPI and AI, facilitate greater carbon accumulation, as identified in the NGBoost-SHAP analysis.

The high SI also signals the vulnerability of carbon stocks to wetland loss, a critical consideration for the transboundary IRB, where land-use pressures and hydrological variability threaten wetland integrity (Sahana et al. 2024). For instance, the projected 39.37% wetland area reduction under the Wetland Degradation Scenario (S3) in 2030 leads to a 35.15% decline in carbon storage (from 2.885×10^8 tC in 2020 to 1.871×10^8 tC), consistent with the SI's implications. Conversely, the Wetland Protection Scenario (S2) demonstrates that a 12.05% wetland area increase could boost carbon storage by 18.59% (to 3.421×10^8 tC), reinforcing the efficacy of conservation policies. These findings align with global strategies to leverage wetlands as natural carbon sinks for climate change mitigation (Davidson and Finlayson 2018). However, the SI's linear assumption may overlook ecological thresholds where carbon storage declines rapidly due to fragmentation or hydrological stress, as suggested by the increased NP. Thus, wetland management in the IRB should prioritize maintaining large, connected wetland patches

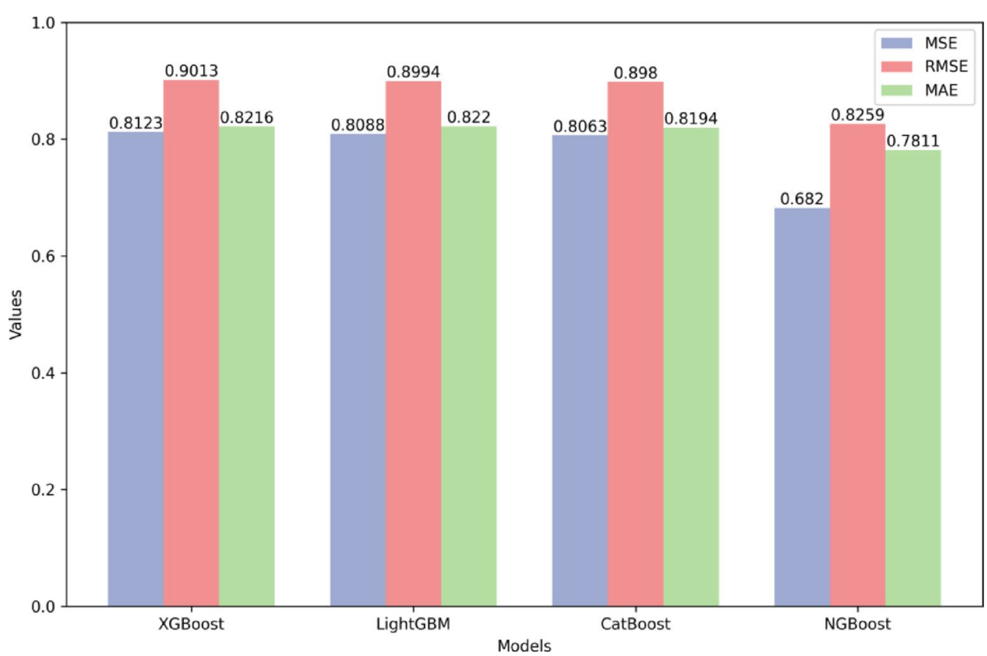

Fig. 7 Comparison of model performance

to maximize carbon sequestration while addressing trans-boundary coordination challenges.

3.4 Feature Importance Analysis Using SHAP

In order to gain a more intuitive understanding of the impact of various landscape patterns on the dynamics of carbon storage in wetlands, we then calculated landscape patterns and carbon stocks for each of the 23 years from 2000 to 2022 (Supplementary Material Table S1). The outcomes represented in Fig. 7 depict the predictive ability of the applied ML algorithms: XGBoost, LightGBM, CatBoost, and NGBoost to identify how different landscape patterns in wetlands affect carbon storage. Interestingly, NGBoost stood out as the most accurate model for this task, with the lowest MSE (0.682), RMSE (0.8259), and MAE (0.7811). This is because the performance of this model can be enhanced by the efficient management of categorical features and the strong gradient boosting methods that the model can adopt to capture the complex patterns between the landscape and carbon storage. From this evaluation, we will derive insights regarding the subsequent SHAP-based analysis that will focus on NGBoost, the top-performing model to comprehend how structure of the landscape affects the stock-disclosure of carbon within the wetlands.

Figure 8 presents the SHAP summary plots for the NGBoost model, illustrating the impact of various landscape pattern indices on carbon storage in the IRB's wetlands. The analysis provides insights into the relative importance and directional influence of each factor. Figure 8(a) displays a sample-wise SHAP summary plot for the landscape pattern indices after generating the NGBoost model, ranked by their contribution. The SHAP value is shown on the x-axis, while the landscape pattern indices are presented on the y-axis. Each point represents a wetland sample, with the color indicating the value of a particular index - blue denoting lower values and red denoting higher values. The horizontal position of each point indicates whether the index influences the prediction positively or negatively.In the NGBoost model, the AI, LPI, and NP emerge as the top three influential factors for carbon storage prediction. AI shows the most significant range of both positive and negative impacts, with higher values (red points) generally having a larger positive influence. LPI also demonstrates a wide range of influence, with higher values typically showing a positive impact. NP, while having a smaller overall impact, shows a broad

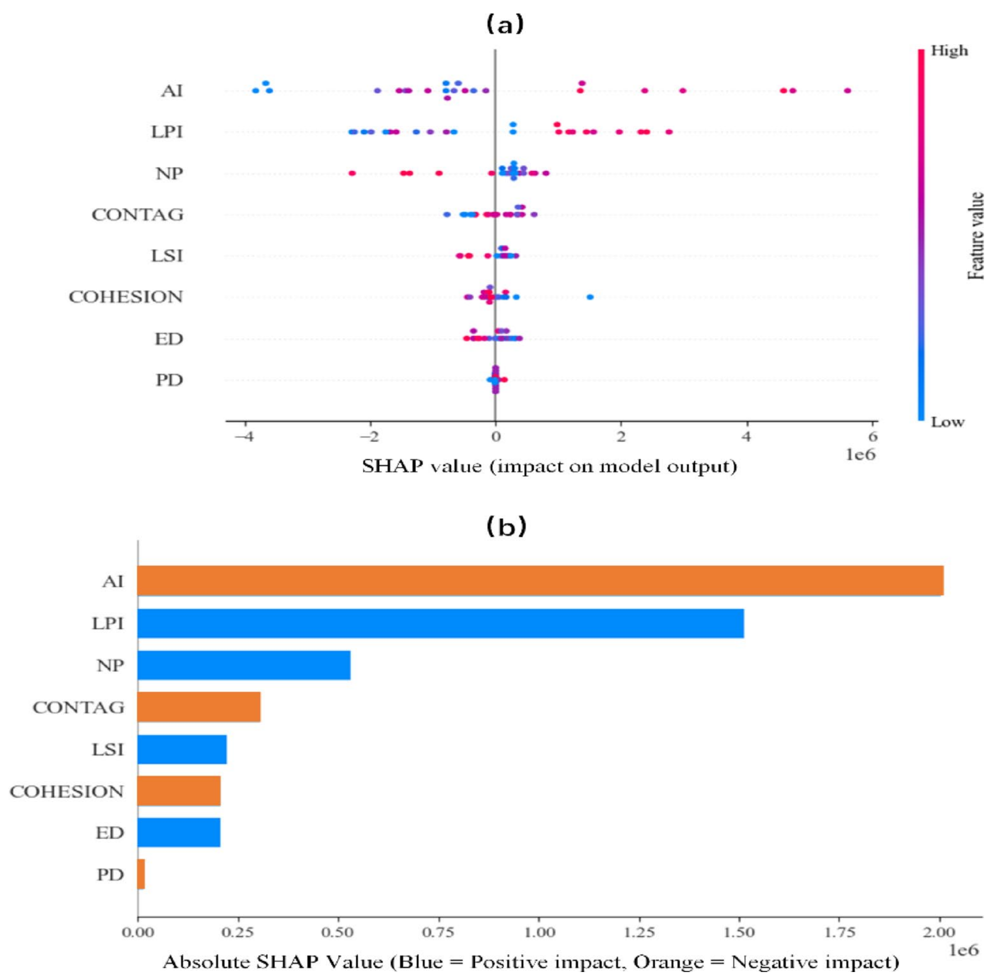

Fig. 8 Local explanation of the NGBoost using SHAP values for entire study area. (**a**) sample-wise SHAP values, (**b**) mean SHAP values for each conditioning factor

distribution of SHAP values. The remaining indices show relatively smaller impacts, with their SHAP values clustered around zero. Figure 8(b) illustrates the mean absolute SHAP values for all input landscape pattern indices. This visualization helps understand the magnitude and direction of each index's overall impact on predicting carbon storage in the study area. The length of each bar represents the absolute mean SHAP value, indicating the overall importance of the index. Blue bars indicate a positive impact, while orange bars represent a negative impact. AI shows the largest mean impact, primarily negative. This suggests that while AI can have strong positive effects on individual samples, its overall tendency is to decrease carbon storage predictions. LPI is the second most influential factor, with a consistently positive impact. NP ranks third in importance, also showing a purely positive influence. CONTAG and COHESION display small negative impacts, while LSI and ED show minor positive influences. PD has the smallest mean impact among all indices.

These SHAP summary plots provide valuable insights into the complex relationships between landscape pattern indices and carbon storage in the IRB's wetlands. They highlight the nuanced roles of landscape aggregation, patch size, and patch number in determining carbon storage potential. The analysis reveals that while increased aggregation (AI) can have varied effects, larger patches (LPI) and a higher number of patches (NP) consistently contribute positively to carbon storage predictions. This information is crucial for understanding the model's behavior and can

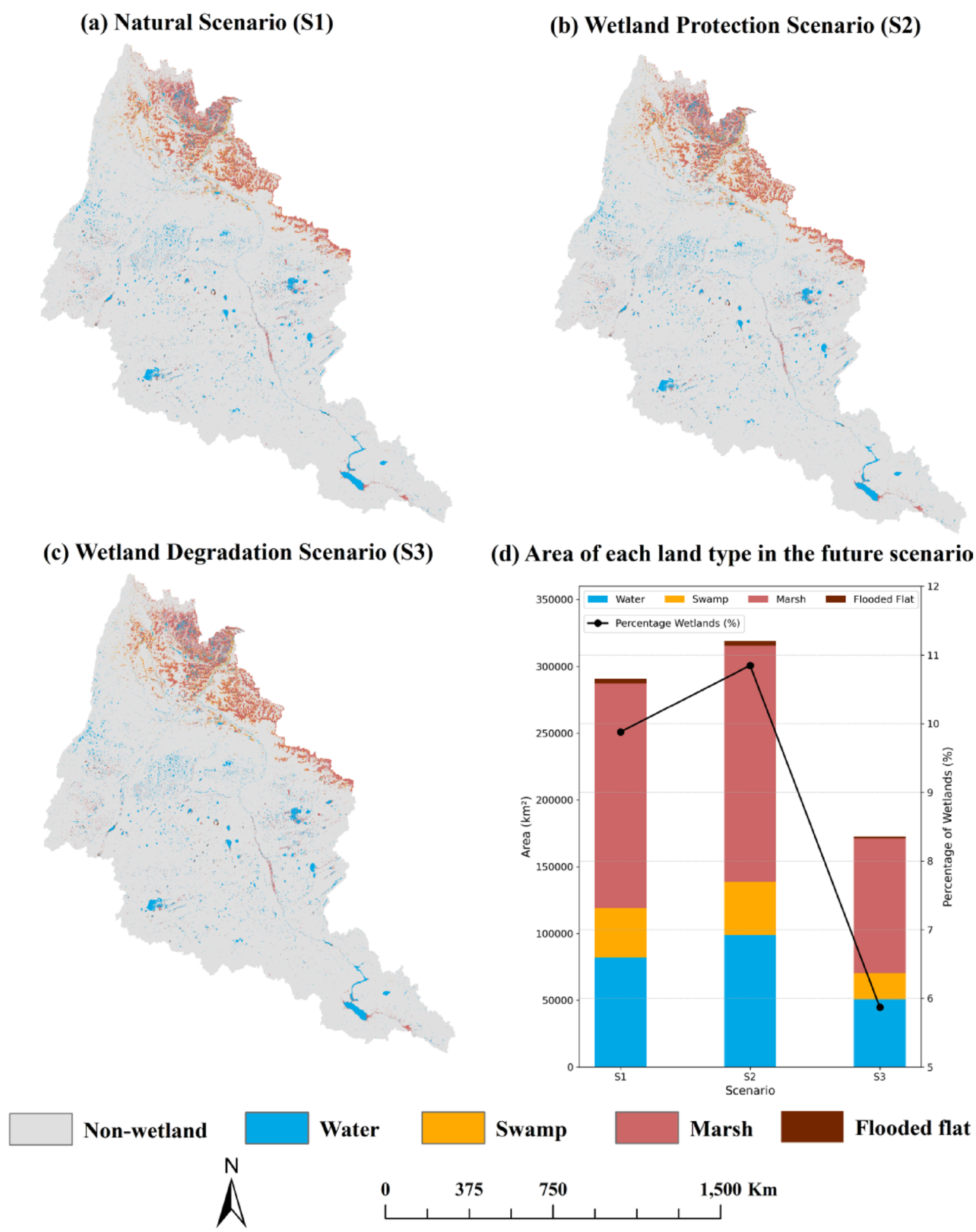

Fig. 9 Land use under different future multi-scenario in 2030

Table 10 Wetland area statistics under 2030 future multi-scenario

Scenario	Wetland area by type(km²)					Total wetland area(km²)	Percentage of wetlands(%)
	Non-wetland	Water	Swamp	Marsh	Flooded flat		
S1	2649507.68	82245.68	36878.09	168246.1217	3344.43	290714.32	9.88
S2	2621130.58	99063.65	39743.16	176717.79	3566.83	319091.42	10.85
S3	2767596.23	50727.61	19799.73	100639.21	1459.23	172625.78	5.87

Table 11 Area changes of different land types in different scenarios from 2020 to 2030

Scenario	Property	Non-wetland	Water	Swamp	Marsh	Flooded flat
S1	Area (km²)	− 5957.38	4275.06	− 4.07	1446.23	300.55
	Dynamic Index (%)	− 0.22	5.48	− 0.17	0.87	9.87
S2	Area (km²)	− 34334.48	21093.03	2801	9917.9	522.95
	Dynamic Index (%)	− 1.29	27.05	7.59	5.95	17.17
S3	Area (km²)	112131.17	− 27243.01	− 17142.43	− 66160.68	− 1584.65
	Dynamic Index (%)	4.22	− 34.94	− 46.4	− 39.67	− 52.05

inform landscape management strategies aimed at optimizing carbon sequestration in wetland ecosystems.

3.5 Analysis of Results of Future Multi-Scenario Projections

The future multi-scenario projections for 2030, simulated using the PLUS model, elucidate the impacts of distinct land-use policies on wetland extent and carbon storage in the IRB (Fig. 9). These scenarios—Natural (S1), Wetland Protection (S2), and Wetland Degradation (S3)—build on the historical trends and sensitivity analysis, offering a forward-looking perspective on how landscape management influences carbon sequestration. The variations across scenarios highlight the interplay between wetland area, landscape structure, and carbon storage, with implications for transboundary conservation strategies.

Table 10 provides detailed wetland area statistics for the different scenarios. In the S1, the total wetland area is 290,714.32 km², accounting for 9.88% of the total land area. This scenario assumes no significant policy interventions, resulting in moderate land-use changes. In contrast, the S2 shows the largest wetland area, at 319,091.42 km², covering 10.85% of the land. This expansion is a direct result of policy-driven wetland restoration and conservation efforts. On the other hand, the S3 results in severe wetland loss, with only 172,625.78 km² of wetlands remaining, making up just 5.87% of the land area. The steep decline in wetland coverage under this scenario reflects the pressures from urbanization and agricultural expansion.

Table 11 highlights the changes in land area by wetland type between 2020 and 2030 for each scenario. In S1, the overall wetland area shows minor changes, with a slight decrease in non-wetland areas, and a modest increase in marshes, which grow by 1,446.23 km² (a 0.87% dynamic index). Water areas also see a moderate increase, gaining 4,275.06 km² (5.48%), while swamp and flooded flat areas remain relatively stable. The S2 scenario, focused on wetland protection, exhibits the most significant gains in wetland area, with water bodies expanding by 21,093.03 km² (27.05%) and marshes increasing by 9,917.9 km² (5.95%). These positive changes reflect the success of conservation policies. Conversely, the S3 scenario results in substantial wetland losses. Marshes suffer the most, losing 66,160.68 km² (a -39.67% dynamic index), followed by swamps, which decline by 17,142.43 km² (-46.4%), and water bodies, which decrease by 27,243.01 km² (-34.94%). This scenario demonstrates the destructive effects of urban and agricultural development on wetlands.

The changes in wetland area are directly linked to the projected carbon storage in 2030, as shown in Fig. 10; Table 12. Under the S1 scenario, total carbon storage reaches 3.229×10^8 tC, with marshes contributing the largest share at 2.272×10^8 tC. Swamps, although smaller in area, also store significant carbon at 8.6296×10^7 tC. The S2 scenario, which prioritizes wetland protection, achieves the highest total carbon storage, at 3.421×10^8 tC. The expanded wetland areas, particularly marshes (2.386×10^8 tC) and swamps (9.2928×10^7 tC), significantly boost the carbon sequestration potential of the IRB. This scenario demonstrates the positive impact of wetland restoration efforts on carbon storage capacity.

In stark contrast, the S3 scenario results in a dramatic reduction in carbon storage, with total carbon sequestration falling to 1.871×10^8 tC. The loss of marsh area, which drops to 1.3589×10^8 tC, accounts for most of the decrease in carbon storage. Swamps and water bodies also contribute less to carbon sequestration in this scenario, reflecting the negative consequences of wetland degradation. The sharp decline in carbon storage under S3 highlights the critical role that wetlands play in carbon sequestration and the dangers posed by unchecked land-use changes.

Collectively, the 2030 projections underscore the pivotal role of policy-driven wetland management in enhancing

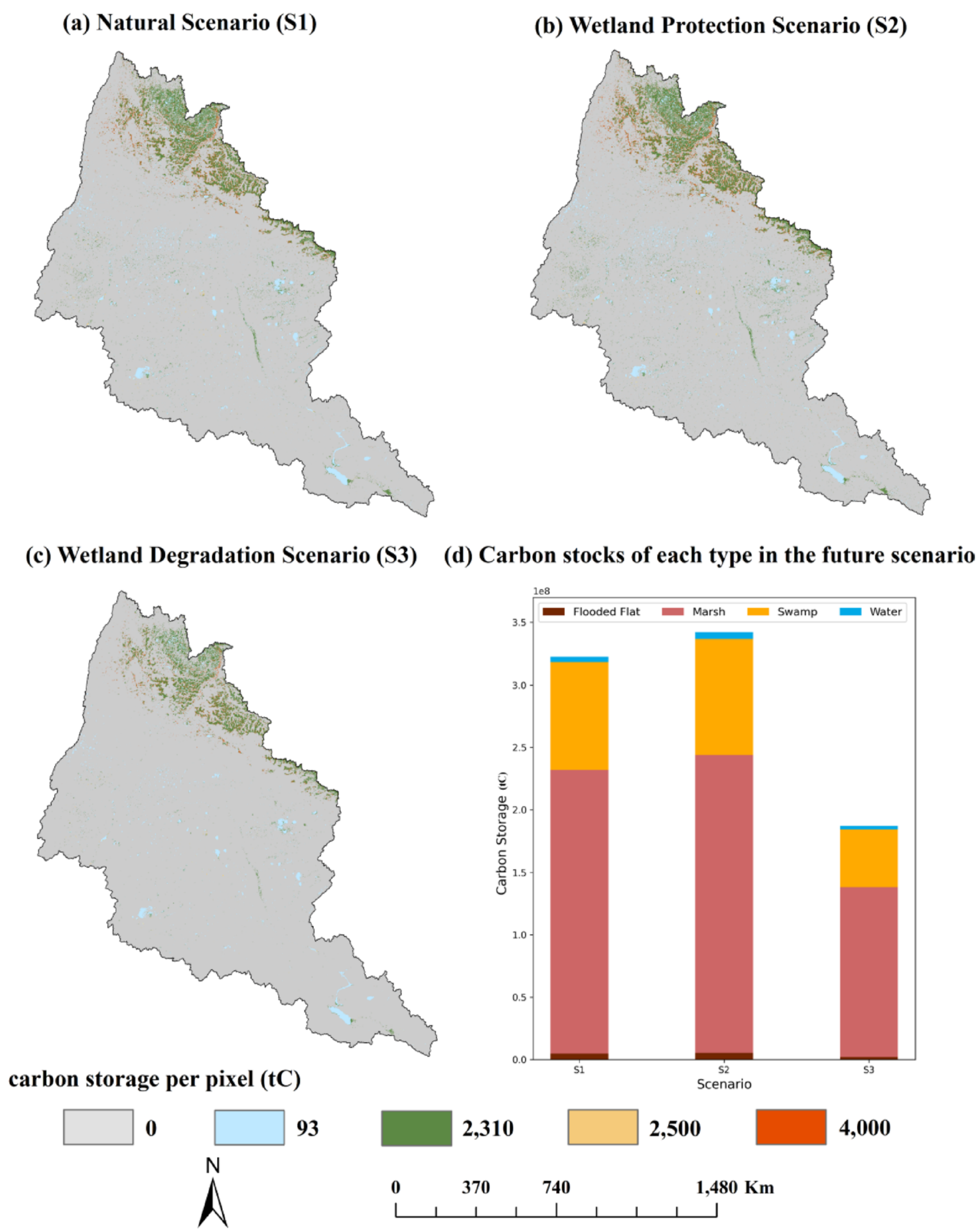

Fig. 10 Carbon stocks under different future multi-scenario in 2030

Table 12 Carbon storage (tC) by wetland type in 2030 future multi-scenario

Scenario	Water	Swamp	Marsh	Flooded flat	Total
S1	4,471,161	86,296,000	227,209,290	4,887,500	322,863,951
S2	5,385,444	92,928,000	238,625,310	5,212,500	342,151,254
S3	2,757,729	46,296,000	135,894,990	2,132,500	187,081,219

carbon sequestration and ecosystem resilience in the IRB. The S2 achieves the highest carbon storage (3.421×10^8 tC) by expanding wetland area to 319,091.42 km², particularly through marsh (+9,917.9 km²) and swamp (+2,801 km²) restoration, aligning with the high sensitivity of carbon storage to wetland area. This scenario leverages landscape features like high LPI and AI, identified as key carbon storage drivers in the NGBoost-SHAP analysis, to maximize sequestration efficiency. In contrast, the S1 maintains stable carbon storage (3.229×10^8 tC) but misses opportunities for significant gains due to limited wetland expansion. The S3, with a drastic reduction to 1.871×10^8 tC and 172,625.78 km² of wetlands, illustrates the severe consequences of unchecked land-use intensification, particularly marsh loss (-66,160.68 km²), which disrupts carbon storage and landscape connectivity. These findings reinforce the need for proactive conservation policies, such as those modeled in S2, to safeguard wetlands as critical carbon sinks and support transboundary climate mitigation efforts (Sahana et al. 2024).

4 Discussion

4.1 Interpretation of Landscape and Carbon Storage Dynamics

The analysis of wetland landscape patterns and carbon storage in the IRB from 2000 to 2020 reveals a notable expansion of wetland coverage, increasing from 274,339.61 km² (9.33% of the total area) to 284,756.56 km² (9.68%), a net gain of 10,416.95 km² (Table 7). This 3.79% increase, primarily driven by swamps (+2,466.52 km²) and water bodies (+6,754.90 km²), contrasts with declines in flooded flats (-2,666.31 km²), suggesting a heterogeneous response to conservation policies and hydrological changes. Compared to other semi-arid regions, such as the Yellow River Delta, where wetland area decreased by 12.4% from 1990 to 2010 due to agricultural expansion (Kong et al. 2020), the IRB's wetland growth reflects effective restoration efforts, possibly linked to China's Grain for Green Project and transboundary conservation initiatives (Zhang et al. 2021). However, unlike the Prairie Pothole Region, where wetland expansion enhanced carbon sequestration uniformly across wetland types (Gleason et al. 2011), the IRB's mixed trends (e.g., flooded flat losses) indicate localized pressures that may limit carbon storage potential. This expansion aligns with increased carbon storage (from 2.827×10^8 tC to 2.885×10^8 tC), underscoring wetlands' role as critical carbon sinks in the IRB.

Landscape pattern indices reveal structural changes in IRB wetlands, with implications for ecological functionality. The NP increased from 15,744 to 16,800, ED rose from 0.4285 to 0.4441 m/ha, and PD grew from 0.0033 to 0.0035 patches/ha (Table 8), indicating progressive fragmentation. This trend mirrors findings in the Sanjiang Plain, China, where wetland fragmentation increased NP by 15% from 1995 to 2015, reducing carbon sequestration efficiency due to edge effects (Liu et al. 2019). In contrast, the IRB's LPI slightly increased from 0.7184 to 0.7933%, suggesting that dominant wetland patches remain intact, similar to stable large patches in the Everglades, which sustain carbon storage despite fragmentation (Liu et al. 2005). The CONTAG decreased marginally from 61.9399 to 61.7163%, and the LSI rose from 132.8145 to 135.0433, reflecting increased spatial complexity, likely due to new, smaller wetland patches (Fickas et al. 2016). However, the COHESION remained stable (99.8940–99.8923%), and the AI slightly increased from 65.6419 to 65.7339%, indicating sustained connectivity, unlike the Danube Delta, where connectivity declined with fragmentation (Nichersu et al. 2022). These patterns suggest that while fragmentation poses risks to carbon sequestration NGBoost-SHAP analysis (AI and LPI as key predictors), the IRB's stable large patches and connectivity mitigate some negative impacts, supporting carbon storage gains (Bridgham et al. 2006).

Regarding carbon storage, the study reveals a positive trend. The total carbon storage in the IRB wetlands increased from 2.827×10^8 tC in 2000 to 2.885×10^8 tC in 2020, representing a net gain of 5.8×10^6 tC over the two-decade period. This increase aligns with the expansion of wetland area, suggesting that the growth in wetland coverage has contributed to enhanced carbon sequestration capacity in the region (Zhang et al. 2023b). The analysis presented in this study reveals the intricate relationship between wetland landscape patterns and carbon storage within the IRB. The observed increase in wetland coverage and the associated rise in carbon storage underscore the significant role these ecosystems play in global carbon cycling. Despite the overall positive trend in wetland expansion, the study also notes a concurrent increase in landscape fragmentation, as indicated by the rising number of patches and edge density. This fragmentation, while not entirely detrimental, suggests a need for careful management to preserve the ecological functions of these wetlands (Nahlik and Fennessy 2016).

4.2 Sensitivity, Model Performance, and Implications for Ecosystem Management

The sensitivity analysis, yielding an SI of 10.812, highlights the acute responsiveness of carbon storage to wetland area changes in the IRB. This high SI indicates that a 1% increase in wetland area amplifies carbon storage by over 10%, driven by the carbon-rich marshes and swamps dominating the IRB (Deng et al. 2022). Compared to the Mississippi River Delta, where an SI of 8.23 was reported for coastal wetlands (DeLaune and White 2012), the IRB's higher sensitivity reflects its semi-arid context, where wetlands are scarce but critical carbon sinks. Similarly, a study in the Poyang Lake Basin found an SI of 9.45, attributing sensitivity to large, connected wetland patches (Wang et al. 2023b; Zhang et al. 2017), aligning with our NGBoost-SHAP findings that emphasize LPI and AI. The IRB's high SI underscores the potential of restoration policies, as seen in the Wetland Protection Scenario (S2), to significantly enhance carbon sequestration, but it also highlights vulnerability to wetland loss, as projected in S3.

The ML analysis, with NGBoost outperforming XGBoost, LightGBM, and CatBoost, demonstrates its efficacy in capturing the complex relationships between landscape patterns and carbon storage. NGBoost's probabilistic approach, which models uncertainty, aligns with its successful application in the Amazon Basin, where it predicted carbon dynamics with 15% lower RMSE than traditional models (Duan et al. 2020). In contrast, a study in the Great Lakes region using Random Forest reported higher errors due to landscape heterogeneity (Basu et al. 2023), suggesting NGBoost's advantage in handling IRB's diverse wetland types. The SHAP analysis identified AI, LPI, and NP as key predictors, consistent with findings in the Chesapeake Bay, where connectivity metrics drove carbon storage predictions (Araza et al. 2023). These results offer actionable insights for IRB management, prioritizing large, aggregated wetland patches to optimize carbon sequestration, as supported by S2's outcomes. However, unlike the Amazon study, which integrated climate variables, our NGBoost model relies on static landscape metrics, potentially limiting its predictive scope (Dorogush et al. 2018).

The SHAP analysis further elucidates the contribution of various landscape indices to carbon storage predictions. The identification of key predictors, such as AI, LPI, and NP, offers actionable insights for targeted management strategies. These findings suggest that enhancing landscape connectivity and preserving large, contiguous wetland patches are crucial for optimizing carbon sequestration. By focusing on these landscape features, managers can develop strategies that not only bolster the carbon storage capacity of wetlands but also support other ecological functions and services (Costanza et al. 1997).

In conclusion, the integration of advanced modeling techniques with sensitivity analysis provides a comprehensive approach to understanding and managing the complex dynamics of wetland ecosystems (Herbert et al. 2021). The results of this study offer a clear direction for ecosystem management in the IRB, emphasizing the need for strategies that prioritize wetland connectivity and area expansion. By doing so, we can harness the full potential of these ecosystems as natural carbon sinks, contributing to regional and global climate change mitigation efforts (Mitsch et al. 2015).

4.3 Insights from Future Multi-Scenario Projections

The PLUS model's 2030 projections for the IRB reveal the critical role of land-use policies in shaping wetland extent and carbon storage, with distinct outcomes across the three scenarios. The S2 scenario, projecting a 12.05% wetland area increase to 319,091.42 km² and a 18.59% carbon storage rise to 3.421×10^8 tC, underscores the efficacy of conservation policies. This aligns with projections for the Mekong Delta, where restoration policies increased wetland area by 10% and carbon storage by 15% by 2030 (Dang et al. 2021). However, unlike the Mekong, where mangrove restoration drove gains, IRB's S2 relies on marsh and swamp expansion, reflecting regional ecological differences (Yin et al. 2024). The S2 outcomes also corroborate the high sensitivity and NGBoost-SHAP findings, emphasizing large, aggregated patches (LPI, AI) as carbon sequestration drivers, similar to the Pantanal's restoration scenarios (Pham et al. 2022). This finding aligns with global trends emphasizing the role of wetlands in climate change mitigation, suggesting that targeted wetland conservation could offer substantial ecological and carbon storage benefits(Davidson and Finlayson 2018).

In contrast, the S3 scenario projects a 39.37% wetland area reduction to 172,625.78 km² and a 35.15% carbon storage decline to 1.871×10^8 tC, driven by urban and agricultural expansion. This mirrors the Yangtze River Basin, where wetland loss of 30% from 2000 to 2020 reduced carbon storage by 25% due to development pressures (Li et al. 2020). Unlike the Yangtze, where regulatory failures exacerbated losses, IRB's transboundary context complicates management, highlighting the need for coordinated policies (Junk et al. 2013). The S1 scenario, maintaining stable wetlands (290,714.32 km²) and carbon storage (3.229×10^8 tC), resembles the Florida Everglades' baseline projections, where limited intervention sustained wetlands but missed restoration gains (An et al. 2025). S1 suggests that without proactive measures, IRB wetlands may not fully leverage their carbon sink potential, as seen in S2. These scenarios emphasize the need for landscape-scale management to balance development and conservation, supporting biodiversity and water regulation alongside carbon sequestration (McGlathery et al. 2007).

The comparative outcomes of these scenarios offer critical insights for policymakers and land managers. They highlight the importance of adopting a long-term, landscape-scale approach to wetland management that accounts for both the immediate and future impacts of land-use decisions. These findings support the argument that strategic wetland protection and restoration are necessary to not only maintain current carbon storage levels but also to enhance the IRB's capacity to act as a regional carbon sink in the face of global climate change (Howard et al. 2017). In addition, the future projections serve as a reminder of the interconnectedness between wetland conservation and broader environmental services. The scenarios emphasize that wetlands play a multifaceted role beyond carbon sequestration, including biodiversity conservation, flood mitigation, and water quality improvement (Zedler and Kercher 2005). Therefore, a comprehensive approach to wetland management that balances these ecosystem services with land-use demands is essential for ensuring the long-term sustainability of the IRB's wetlands (Kirwan and Mudd 2012).

4.4 Limitations and Future Research Directions

This study integrates advanced tools to assess wetland dynamics and carbon storage in the IRB, but limitations in data and methods must be acknowledged. The GWL_FCS30 dataset's 30 m resolution may underestimate small wetland patches and linear features, while mixed pixels at patch boundaries contribute to classification ambiguity. With an 86% accuracy, misclassifications (e.g., confusing wetland types) can propagate through InVEST's carbon storage estimates and landscape metrics, affecting model reliability (He et al. 2016). Similarly, the application of the InVEST model relies on fixed carbon density values for each land use type (Table 3), primarily sourced from existing literature (Schneider et al. 2010). This approach, while necessary for large-scale assessment due to data constraints, inherently simplifies the complex reality of carbon storage dynamics. The IRB encompasses considerable environmental gradients, leading to potential spatial variations in soil organic carbon, biomass, and necromass within the same wetland classification (e.g., marsh, swamp) that are not captured by using single average values. Consequently, the model's outputs represent estimations of carbon stocks, and their absolute accuracy is subject to uncertainties stemming from the generalization of these carbon density parameters. While the relative spatial patterns and temporal changes identified are robust for understanding regional dynamics, refining the absolute quantification would necessitate extensive, basin-specific field measurements to calibrate carbon densities for the diverse local conditions.

The ML and sensitivity analyses also have constraints. NGBoost relies on assumed probability distributions for uncertainty modeling, and its performance is sensitive to hyperparameter tuning, potentially affecting probabilistic forecast accuracy. SHAP, while interpretable, is computationally intensive and may be confounded by correlations among landscape metrics (e.g., AI, LPI), complicating importance attribution (Lundberg and Lee 2017). These factors limit the causal inference of ML results, requiring careful interpretation of driver rankings. SI quantifies average responsiveness but does not detect non-linear responses or ecological thresholds, which are critical in stressed systems like the IRB's wetlands (Zhou et al. 2024a).

Ecological thresholds, dynamic feature importance, climate change, transboundary coordination, co-benefits, and long-term monitoring pose challenges to the study's projections. The SI assumes linear responses, potentially missing thresholds where carbon storage declines rapidly due to wetland loss or fragmentation. SHAP's feature importance, based on 2000–2020 data, may shift under future scenarios; for instance, fragmentation metrics may dominate in degradation scenarios (S3), while largest patch index may be critical in protection scenarios (S2). The PLUS model's 2030 projections, driven by historical trends and socio-economic factors, do not fully integrate climate change effects like precipitation or temperature shifts, which could reduce wetland area and carbon storage in the IRB's semi-arid climate(Zhu et al. 2024). Similarly, the study underutilizes InVEST and NGBoost for transboundary coordination, co-benefits like biodiversity and water quality, and long-term monitoring, despite their potential to provide standardized assessments and driver insights for stakeholders across China, Kazakhstan, and Russia. Data gaps, such as coarse-resolution imagery and uncalibrated carbon densities, further limit model validation and application to carbon markets and payments for ecosystem services (PES). Wetland restoration, as modeled in S2, can enhance carbon sequestration, biodiversity, and water quality, supporting coordinated management (Li et al. 2024b).

Future research should address these limitations to improve projections and management. Higher-resolution imagery (e.g., Sentinel-2, LiDAR) and advanced classification (e.g., OBIA, deep learning) could enhance wetland delineation. Locally calibrated carbon density values, derived from soil and vegetation surveys, would refine InVEST's estimates. For ML, sensitivity analyses of NGBoost distributions and SHAP's robustness to feature correlations are needed. Time-series or scenario-specific sensitivity analyses could detect thresholds, while SHAP applied to future landscapes would clarify dynamic feature importance. Integrating climate variables into PLUS modeling would improve 2030 projections. Long-term monitoring of wetland area, carbon storage, landscape patterns, biodiversity, and water quality, using annual remote sensing and seasonal field measurements, could validate projections (Fluet-Chouinard et al. 2023). Cross-boundary data-sharing platforms could standardize monitoring across IRB countries, supporting stakeholder workshops and PES programs(Chen et al. 2023). Enhanced data collection, integrating dynamic climate data and ground-truth biodiversity metrics, would improve InVEST and NGBoost accuracy, informing joint agreements and sustainable wetland management (Huang et al. 2024).

5 Conclusions

This study provides a comprehensive analysis of the relationship between wetland landscape patterns and carbon storage in the IRB, combining both historical trends from 2000 to 2020 and future projections for 2030 under multiple land-use scenarios. Several significant findings emerge from this research:

(1) The observed increase in wetland coverage from 9.33 to 9.69% of the total land area from 2000 to 2020 corresponds with a substantial rise in carbon storage, from 2.827×10^8 tC to 2.885×10^8 tC. This increase is particularly pronounced in marshes and swamps, which are the dominant wetland types in the region, highlighting their critical role as carbon sinks.

(2) Despite the overall expansion of wetlands, the study also documents an increase in landscape fragmentation, as evidenced by the rising NP and ED. However, the LPI and CONTAG suggest that while fragmentation is occurring, the largest and most contiguous wetland patches remain significant for carbon sequestration.

(3) The SI of 10.812 indicates a strong positive response of carbon storage to changes in wetland area. This suggests that even small changes in wetland extent can have significant impacts on carbon sequestration, emphasizing the need for proactive wetland management and conservation strategies.

(4) The NGBoost model's exceptional predictive performance, characterized by an MSE of 0.682, RMSE of 0.8259, and MAE of 0.7811, underscores its efficacy in elucidating the landscape's response to carbon storage. The SHAP analysis, in particular, has delineated the AI, LPI, and NP as the most influential predictors, offering a targeted basis for enhancing the carbon sequestration efficacy of wetland landscapes.

(5) The 2030 multi-scenario projections show that policy-driven conservation efforts are key to preserving wetland areas and maximizing carbon storage in the IRB. Under the Natural Scenario (S1), carbon storage remains stable at 3.229×10^8 tC. The Wetland Protection Scenario (S2) leads to the highest carbon storage at 3.421×10^8 tC, while the Wetland Degradation Scenario (S3) shows a sharp decline to 1.871×10^8 tC. These findings highlight the importance of conservation policies in mitigating climate change impacts.

These conclusions provide a foundation for future efforts to manage and conserve wetlands in the IRB and similar ecosystems globally. By understanding the specific landscape features that enhance carbon sequestration and acknowledging the critical role of proactive conservation strategies, managers and policymakers can implement more effective wetland management practices that align with broader environmental and climate objectives. The integration of historical analysis with future scenario projections further emphasizes the need for sustainable land-use planning to protect wetlands and their capacity to function as vital carbon sinks in the face of global climate challenges.

Supplementary Information The online version contains supplementary material available at https://doi.org/10.1007/s41748-025-00656-5.

Acknowledgements The authors are particularly grateful to all researchers and institutions for providing data support for this study. We also express our appreciation to the editors and reviewers for their valuable comments, which significantly improved the quality of this manuscript. This research was supported by the Western Young Scholars Project of the Chinese Academy of Sciences (Grant No. 2022-XBQNXZ-001), the Third Xinjiang Comprehensive Scientific Investigation Project (Grant No. 2022xjkk0702), the Tianshan Talent Development Program (Grant No. 2022TSYCCX0006), and the Chinese Academy of Sciences President's International Fellowship Initiative (Grant No. 2024PVB0064).

Author Contributions All authors contributed to the study conception and design. Kaiyue Luo and Alim Samat were responsible for the conceptualization and methodology. Kaiyue Luo conducted the investigation, visualization, and data curation, and wrote the original draft. Alim Samat provided supervision, funding acquisition, and project administration. Tim Van de Voorde and Weiguo Jiang contributed to the methodology and writing– review & editing. Jilili Abuduwaili provided supervision, funding acquisition, and project administration. All authors read and approved the final manuscript.

Funding This research was funded by the Western Young Scholars Project of the Chinese Academy of Sciences (Grant No. 2022-XBQNXZ-001), the Third Xinjiang Comprehensive Scientific Investigation Project (Grant No. 2022xjkk0702), the Tianshan Talent Development Program (Grant No. 2022TSYCCX0006), and the Chinese Academy of Sciences President's International Fellowship Initiative (Grant No. 2024PVB0064).

Declarations

Competing Interests The authors have no relevant financial or non-financial interests to disclose.

References

Abatzoglou JT, Dobrowski SZ, Parks SA, Hegewisch KC (2018) TerraClimate, a high-resolution global dataset of monthly climate and Climatic water balance from 1958–2015. Sci Data 5:1–12

An X, Zhang M, Zhang H, Liu Y (2025) Spatiotemporal changes and driving mechanisms of carbon stocks in the Yangtze river basin of China over the past 20 years. Adv Space Res 75:53–73

Araza A, De Bruin S, Hein L, Herold M (2023) Spatial predictions and uncertainties of forest carbon fluxes for carbon accounting. Sci Rep 13:12704

Basu NB, Dony J, Van Meter K, Johnston SJ, Layton AT (2023) A random forest in the great lakes: Stream nutrient concentrations

across the transboundary great lakes basin. *Earth's Future*, 11, e2021EF002571
Bellard C, Bertelsmeier C, Leadley P, Thuiller W, Courchamp F (2012) Impacts of climate change on the future of biodiversity. Ecol Lett 15:365–377
Bridgham SD, Megonigal JP, Keller JK, Bliss NB, Trettin C (2006) The carbon balance of North American wetlands. Wetlands 26:889–916
Chaplin-Kramer R, Polasky S, Alkemade R, Burgess ND, Cheung WW, Fetzer I, Harfoot M, Hertel TW, Hill SL, Johnson JA (2024) Integrated modeling of Nature's role in human well-being: A research agenda. Glob Environ Change 88:102891
Chen Z, Yu B, Yang C, Zhou Y, Qian X, Wang C, Wu B, Wu J (2020) An extended time-series (2000–2018) of global NPP-VIIRS-like nighttime light data from a cross-sensor calibration. *Earth System Science Data Discussions*, 2020, 1–34
Chen J, Gao M, Cheng S, Hou W, Song M, Liu X, Liu Y (2022a) Global 1 Km× 1 Km gridded revised real gross domestic product and electricity consumption during 1992–2019 based on calibrated nighttime light data. Sci Data 9:202
Chen Y, Han Q, Liu G, Wu Y, Li K, Hong J (2022b) Determining critical success factors of urban renewal projects: multiple integrated approach. J Urban Plan Dev 148:04021058
Chen W, Wang J, Ding J, Ge X, Han L, Qin S (2023) Detecting long-term series eco-environmental quality changes and driving factors using the remote sensing ecological index with salinity adaptability (RSEISI): a case study in the Tarim river basin, China. Land 12:1309
Chmura GL, Anisfeld SC, Cahoon DR, Lynch JC (2003) Global carbon sequestration in tidal, saline wetland soils. Glob Biogeochem Cycles, 17
Chu W, Zhang C, Li H, Zhang L, Shen D, Li R (2024) SHAP-powered insights into Spatiotemporal effects: unlocking explainable Bayesian-neural-network urban flood forecasting. Int J Appl Earth Obs Geoinf 131:103972
Costanza R, D'arge R, De Groot R, Farber S, Grasso M, Hannon B, Limburg K, Naeem S, O'neill RV, Paruelo J (1997) The value of the world's ecosystem services and natural capital. Nature 387:253–260
Dang AT, Kumar L, Reid M, Nguyen H (2021) Remote sensing approach for monitoring coastal wetland in the Mekong delta, Vietnam: change trends and their driving forces. Remote Sens 13:3359
Davidson NC (2014) How much wetland has the world lost? Long-term and recent trends in global wetland area. Mar Freshw Res 65:934–941
Davidson NC, Finlayson CM (2018) Extent, regional distribution and changes in area of different classes of wetland. Mar Freshw Res 69:1525–1533
DE, Araújo WS, SILVEIRA LT (2024) Ecological networks in savannas reflect different levels of hydric stress in adjacent palm swamp forest ecosystems. Sci Rep 14:21317
Delaune R, White JR (2012) Will coastal wetlands continue to sequester carbon in response to an increase in global sea level? A case study of the rapidly subsiding Mississippi river deltaic plain. Clim Change 110:297–314
Deng Y, Jiang W, Wu Z, Peng K, Ling Z, Li Z, Wang X (2022) Assessing and characterizing carbon storage in wetlands of the Guangdong–Hong Kong–Macau greater Bay area, China, during 1995–2020. IEEE J Sel Top Appl Earth Observations Remote Sens 15:6110–6120
Dorogush AV, Ershov V, Gulin A (2018) CatBoost: gradient boosting with categorical features support. *arXiv preprint arXiv:1810.11363*
Du C, Ge S, Song P, Jombach S, Fekete A, Valánszki I (2025) Optimizing urban green spaces for Vegetation-Based carbon sequestration: the role of landscape Spatial structure in Zhengzhou parks, China. Forests 16:679
Duan T, Anand A, Ding DY, Thai KK, Basu S, Ng A, Schuler A (2020) Ngboost: natural gradient boosting for probabilistic prediction. Int Conf Mach Learn PMLR:2690–2700
Erwin KL (2009) Wetlands and global climate change: the role of wetland restoration in a changing world. Wetlands Ecol Manage 17:71–84
Fan L, Cai T, Wen Q, Han J, Wang S, Wang J, Yin C (2023) Scenario simulation of land use change and carbon storage response in Henan Province, China: 1990–2050. Ecol Ind 154:110660
Fickas KC, Cohen WB, Yang Z (2016) Landsat-based monitoring of annual wetland change in the Willamette Valley of Oregon, USA from 1972 to 2012. Wetlands Ecol Manage 24:73–92
Fluet-Chouinard E, Stocker BD, Zhang Z, Malhotra A, Melton JR, Poulter B, Kaplan JO, Goldewijk KK, Siebert S, Minayeva T (2023) Extensive global wetland loss over the past three centuries. Nature 614:281–286
Gardner RC, Finlayson C (2018) Global wetland outlook: state of the world's wetlands and their services to people. Ramsar convention secretariat, pp 2020–2025
Gleason RA, Euliss N Jr, Tangen B, Laubhan M, Browne B (2011) USDA conservation program and practice effects on wetland ecosystem services in the prairie pothole region. Ecol Appl 21:S65–S81
Guo W, Teng Y, Li J, Yan Y, Zhao C, Li Y, Li X (2024) A new assessment framework to forecast land use and carbon storage under different SSP-RCP scenarios in China. Sci Total Environ 912:169088
Guthrie AG, Bilkovic DM, Mitchell M, Chambers R, Thompson JS, Isdell RE (2022) Ecological equivalency of living shorelines and natural marshes for fish and crustacean communities. Ecol Eng 176:106511
Hamel P, Guerry A, Polasky S, Han B, Douglass J, Hamann M, Janke B, Kuiper J, Levrel H, Liu H (2021) Mapping the benefits of nature in cities with the invest software. Npj Urban Sustain 1:25
He C, Zhang D, Huang Q, Zhao Y (2016) Assessing the potential impacts of urban expansion on regional carbon storage by linking the LUSD-urban and invest models. Environ Model Softw 75:44–58
Herbert ER, Windham-Myers L, Kirwan ML (2021) Sea-level rise enhances carbon accumulation in united States tidal wetlands. One Earth 4:425–433
Hou X, Song B, Zhang X, Wang X, Li D (2024a) Multi-scenario simulation and Spatial-temporal analysis of LUCC in China's coastal zone based on coupled SD-FLUS model. Chin Geogra Sci 34:579–598
Hou Y, Wang L, Li Z, Ouyang X, Xiao T, Wang H, Li W, Nie X (2024b) Landscape fragmentation and regularity lead to decreased carbon stocks in basins: evidence from century-scale research. J Environ Manage 367:121937
Howard J, Sutton-Grier A, Herr D, Kleypas J, Landis E, Mcleod E, Pidgeon E, Simpson S (2017) Clarifying the role of coastal and marine systems in climate mitigation. Front Ecol Environ 15:42–50
Huang F, Xia Z, Li F, Guo L, Yang F (2012) Hydrological changes of the Irtysh river and the possible causes. Water Resour Manage 26:3195–3208
Huang F, Xia Z-Q, Guo L-D, Yang F-C (2014) Effects of reservoirs on seasonal discharge of Irtysh river measured by Lepage test. Water Sci Eng 7:363–372
Huang Z, Li S, Peng J, Ma X, Ding H, Cheng F, Bi R (2024) Assessing ecosystem service dynamics and drivers for sustainable management in the Agro-pastoral ecotone of Northern China: A Spatiotemporal analysis. Ecol Ind 165:112213

in the cold climate– a systematic review of Irtysh River. *Journal of Hydrology: Regional Studies* 42, 101173

Jia Y, Tang L, Xu M, Yang X (2019) Landscape pattern indices for evaluating urban Spatial morphology–A case study of Chinese cities. Ecol Ind 99:27–37

Jiang S, Yuan Y, Chen F, Shang H, Zhang T, Yu S, Qin L, Zhang R (2016) A 291 year precipitation reconstruction in the upper Irtysh river basin based on tree-ring width. Acta Ecol Sin 36:2866–2875

Junk WJ, An S, Finlayson C, Gopal B, Květ J, Mitchell SA, Mitsch WJ, Robarts RD (2013) Current state of knowledge regarding the world's wetlands and their future under global climate change: a synthesis. Aquat Sci 75:151–167

Ke G, Meng Q, Finley T, Wang T, Chen W, Ma W, Ye Q, Liu T-Y (2017) Lightgbm: A highly efficient gradient boosting decision tree. Adv Neural Inf Process Syst, 30

Kirwan ML, Mudd SM (2012) Response of salt-marsh carbon accumulation to climate change. Nature 489:550–553

Kong X, Li Y, Han M, Tian L, Niu X, Zhu J, Wang M, Huang S (2020) Distribution of natural wetlands in the yellow river Delta for three periods since 1990 and driving factors of their changes. Wetl Sci 18:603–612

Lai Y, Sun W, Schmöcker J-D, Fukuda K, Axhausen KW (2023) Explaining a century of Swiss regional development by deep learning and SHAP values. Environ Plann B: Urban Analytics City Sci 50:2238–2253

Li X, Zhou W, Ouyang Z, Xu W, Zheng H (2012) Spatial pattern of greenspace affects land surface temperature: evidence from the heavily urbanized Beijing metropolitan area, China. Landscape Ecol 27:887–898

Li X, Liu B, Wang Y, Yang Y, Liang R, Peng F, Xue S, Zhu Z, Li K (2020) Hydrodynamic and environmental characteristics of a tributary Bay influenced by backwater jacking and intrusions from a main reservoir. Hydrol Earth Syst Sci 24:5057–5076

Li M, Abuduwaili J, Liu W, Feng S, Saparov G, Ma L (2024a) Application of geographical detector and geographically weighted regression for assessing landscape ecological risk in the Irtysh river basin, central Asia. Ecol Ind 158:111540

Li W, Samat A, Abuduwaili J, Wang W (2024b) Spatiotemporal pattern, evolutionary trend, and driving forces analysis of ecological quality in the Irtysh river basin (2000–2020). Land 13:222

Liang X, Liu X, Li D, Zhao H, Chen G (2018) Urban growth simulation by incorporating planning policies into a CA-based future land-use simulation model. Int J Geogr Inf Sci 32:2294–2316

Liu H, Lü X, Zhang S-K, Yang Q (2005) Fragmentation process of wetland landscape in watersheds of Sanjiang plain, China. *Ying Yong Sheng Tai Xue bao = the*. J Appl Ecol 16:289–295

Liu S-Y, Hu N-K, Zhang J, Lv Z-C (2018) Spatiotemporal change of carbon storage in the Loess Plateau of northern Shaanxi, based on the invest model

Liu X, Wang S, Wu P, Feng K, Hubacek K, Li X, Sun L (2019) Impacts of urban expansion on terrestrial carbon storage in China. Environ Sci Technol 53:6834–6844

Lundberg SM, Lee S-I (2017) A unified approach to interpreting model predictions. Adv Neural Inf Process Syst, 30

Luo K, Samat A, Abuduwaili J, Li W (2023) Evaluation of remote sensing products for wetland mapping in the Irtysh river basin. Geosciences 14:14

Maxwell SL, Reside A, Trezise J, Mcalpine CA, Watson JE (2019) Retention and restoration priorities for climate adaptation in a multi-use landscape. Global Ecol Conserv 18:e00649

Mcgarigal K, Cushman SA, Neel MC, Ene E (2002) Fragstats: spatial pattern analysis program for categorical maps. *Computer software program produced by the authors at the University of Massachusetts, Amherst. Available at the following web site*: www.umass.edu/landeco/research/fragstats/fragstats. *html*, 6

Mcglathery KJ, Sundbäck K, Anderson IC (2007) Eutrophication in shallow coastal Bays and lagoons: the role of plants in the coastal filter. Mar Ecol Prog Ser 348:1–18

Meng B, Li M, Du X, Ye X (2022) Flood control and aquifer recharge effects of sponge City: A case study in North China. Water 14:92

Mitsch WJ, Bernal B, Hernandez ME (2015) Ecosystem services of wetlands. Taylor & Francis

Murray NJ (2023) The extent and drivers of global wetland loss. Nature Publishing Group UK London

Nahlik AM, Fennessy MS (2016) Carbon storage in US wetlands. Nat Commun 7:1–9

Nath B, Niu Z, Singh RP (2018) Land use and land cover changes, and environment and risk evaluation of Dujiangyan City (SW China) using remote sensing and GIS techniques. Sustainability 10:4631

Nelson E, Mendoza G, Regetz J, Polasky S, Tallis H, Cameron D, Chan KM, Daily GC, Goldstein J, Kareiva PM (2009) Modeling multiple ecosystem services, biodiversity conservation, commodity production, and tradeoffs at landscape scales. Front Ecol Environ 7:4–11

Nichersu I, Nichersu I, Constantinescu A, Nichersu A (2022) A transdisciplinary approach using Danube river Multi-connectivity in wetland management. The lower Danube river: Hydro-Environmental issues and sustainability. Springer

Osland MJ, Feher LC, Griffith KT, Cavanaugh KC, Enwright NM, Day RH, Stagg CL, Krauss KW, Howard RJ, Grace JB (2017) Climatic controls on the global distribution, abundance, and species richness of Mangrove forests. Ecol Monogr 87:341–359

Peng K, Jiang W, Ling Z, Hou P, Deng Y (2021) Evaluating the potential impacts of land use changes on ecosystem service value under multiple scenarios in support of SDG reporting: A case study of the Wuhan urban agglomeration. J Clean Prod 307:127321

Pham T, Vien N, Vo Q, Tang T, Nguyen T, Tran N, Nguyen T, Nguyen T, Nguyen N (2022) Opportunities and challenges for Mangrove restoration in the Mekong delta: status, policies and stakeholder outlook

Polasky S, Nelson E, Pennington D, Johnson KA (2011) The impact of land-use change on ecosystem services, biodiversity and returns to landowners: a case study in the state of Minnesota. Environ Resource Econ 48:219–242

Prokhorenkova L, Gusev G, Vorobev A, Dorogush AV, Gulin A (2018) CatBoost: unbiased boosting with categorical features. Adv Neural Inf Process Syst, 31

Qiu H, Hu B, Zhang Z (2021) Impacts of land use change on ecosystem service value based on SDGs report–Taking Guangxi as an example. Ecol Ind 133:108366

Qiu B, Zhou M, Qiu Y, Liu S, Ou G, Ma C, Tu J, Li S (2022) An integrated Spatial autoregressive model for analyzing and simulating urban Spatial growth in a garden City, China. Int J Environ Res Public Health 19:11732

Radelyuk I, Zhang L, Assanov D, Maratova G, Tussupova K (2022) A state-of-the-art and future perspectives of transboundary rivers

Rogers K, Kelleway JJ, Saintilan N, Megonigal JP, Adams JB, Holmquist JR, Lu M, Schile-Beers L, Zawadzki A, Mazumder D (2019) Wetland carbon storage controlled by millennial-scale variation in relative sea-level rise. Nature 567:91–95

Sahana M, Dhali MK, Lindley S (2024) Global disparities in transboundary river research have implications for sustainable management. Commun Earth Environ 5:786

Schneider A, Friedl MA, Potere D (2010) Mapping global urban areas using MODIS 500-m data: new methods and datasets based on 'urban ecoregions'. Remote Sens Environ 114:1733–1746

Sharp R, Tallis H, Ricketts T, Guerry A, Wood S, Chaplin-Kramer R, Nelson E, Ennaanay D, Wolny S, Olwero N (2015) InVEST Version 3.2. 0 User's Guide. The Natural Capital Project. The Nature Conservancy, and World Wildlife Fund. Stanford University, University of Minnesota

Sorichetta A, Hornby GM, Stevens FR, Gaughan AE, Linard C, Tatem AJ (2015) High-resolution gridded population datasets for Latin America and the Caribbean in 2010, 2015, and 2020. Sci Data 2:1–12

Stupariu M-S, Cushman SA, Pleşoianu A-I, Pătru-Stupariu I, Fuerst C (2022) Machine learning in landscape ecological analysis: a review of recent approaches. Landscape Ecol 37:1227–1250

Turner MG (1989) Landscape ecology: the effect of pattern on process. Annu Rev Ecol Syst, 171–197

Van Asselen S, Verburg PH (2013) Land cover change or land-use intensification: simulating land system change with a global-scale land change model. Glob Change Biol 19:3648–3667

Verburg PH, Schot PP, Dijst MJ, Veldkamp A (2004) Land use change modelling: current practice and research priorities. GeoJournal 61:309–324

Villa JA, Bernal B (2018) Carbon sequestration in wetlands, from science to practice: an overview of the biogeochemical process, measurement methods, and policy framework. Ecol Eng 114:115–128

Wang Y, Li X, Zhang Q, Li J, Zhou X (2018) Projections of future land use changes: multiple scenarios-based impacts analysis on ecosystem services for Wuhan City, China. Ecol Ind 94:430–445

Wang R, Ding J, Ge X, Wang J, Qin S, Tan J, Han L, Zhang Z (2023a) Impacts of climate change on the wetlands in the arid region of Northwestern China over the past 2 decades. Ecol Ind 149:110168

Wang Y, Zhang Z, Chen X (2023b) Land use transitions and the associated impacts on carbon storage in the Poyang lake basin, China. Remote Sens 15:2703

Wang J, Yu G, Han L, Yao Y, Sun M, Yan Z (2024) Ecosystem carbon exchange across China's coastal wetlands: Spatial patterns, mechanisms, and magnitudes. Agric for Meteorol 345:109859

Woo M-K, Thorne R, Szeto K, Yang D (2008) Streamflow hydrology in the boreal region under the influences of climate and human interference. Philosophical Trans Royal Soc B: Biol Sci 363:2249–2258

Wu F (1998) SimLand: a prototype to simulate land conversion through the integrated GIS and CA with AHP-derived transition rules. Int J Geogr Inf Sci 12:63–82

Xiaomin Z, Dongmei Z, Wei Z (2023) Effects of human activities on carbon storage in the Irtysh river basin. Arid Zone Res 40:1333–1345

Xu T, Gao J, Coco G (2019a) Simulation of urban expansion via integrating artificial neural network with Markov chain–cellular automata. Int J Geogr Inf Sci 33:1960–1983

Yin Y, Yang R, Song Z, Lu Y, Zhang Y, Zhang L, Sun M, Li X (2024) Simulation of wetland carbon storage in coastal cities under the coupled framework of socio-economic and ecological sustainability: A case study of Dongying City. Sustainable Cities Soc 108:105481

Yuan Y, Guo W, Tang S, Zhang J (2024) Effects of patterns of urban green-blue landscape on carbon sequestration using XGBoost-SHAP model. J Clean Prod 476:143640

Zedler JB, Kercher S (2005) Wetland resources: status, trends, ecosystem services, and restorability. Annu Rev Environ Resour 30:39–74

Zhang F, Zhan J, Zhang Q, Yao L, Liu W (2017) Impacts of land use/cover change on terrestrial carbon stocks in Uganda. Phys Chem Earth Parts A/B/C 101:195–203

Zhang Z, Fluet-Chouinard E, Jensen K, Mcdonald K, Hugelius G, Gumbricht T, Carroll M, Prigent C, Bartsch A, Poulter B (2021) Development of the global dataset of wetland area and dynamics for methane modeling (WAD2M). Earth Syst Sci Data 13:2001–2023

Zhang X, Liu L, Zhao T, Chen X, Lin S, Wang J, Mi J, Liu W (2023a) GWL_FCS30: a global 30 m wetland map with a fine classification system using multi-sourced and time-series remote sensing imagery in 2020. Earth Syst Sci Data 15:265–293

Zhang Z, Jiang W, Peng K, Wu Z, Ling Z, Li Z (2023b) Assessment of the impact of wetland changes on carbon storage in coastal urban agglomerations from 1990 to 2035 in support of SDG15. 1. Sci Total Environ 877:162824

Zhang X, Liu L, Zhao T, Wang J, Liu W, Chen X (2024) Global annual wetland dataset at 30 m with a fine classification system from 2000 to 2022. Sci Data 11:310

Zhou G, Mao L, Bao T, Zhuang F (2024b) Machine learning-driven CO2 emission forecasting for light-duty vehicles in China. Transp Res Part D: Transp Environ 137:104502

Zhu X, Qie R, Luo C, Zhang W (2024) Assessment and driving factors of wetland ecosystem service function in Northeast China based on InVEST-PLUS model. Water 16:2153